American Mineralogist, Volume 75, pages 886–908, 1990

Manganese, ferric iron, and the equilibrium between garnet and biotite

Michael L. Williams
Department of Geology and Geography, University of Massachusetts, Amherst, Massachusetts 01003, U.S.A.
Jeffrey A. Grambling
Department of Geology, University of New Mexico, Albuquerque, New Mexico 87131, U.S.A.

Abstract

Garnets from the Proterozoic rocks of northern New Mexico vary widely in Mn content but contain very little Ca. In specimens collected from three small areas, X_{sps} in garnet varies from nearly zero to 0.76. Biotite and Fe-Ti oxides occur in each specimen; their compositions change systematically with X_{sps}. After corrections are made for Fe^{3+} in biotite, garnet and biotite show several compositional relationships critical to understanding their equilibrium. K_D (Fe-Mg, garnet-biotite) varies as a function X_{sps} in garnet, but this relationship alone does not constrain the mixing behavior of Mn in garnet because the data show strong linear dependencies among most compositional variables. The most important covariances occur among X_{sps}, $(X_{alm} - X_{prp})$, $(X_{Fe} - X_{Mg})^{Bt}$, X_{Ti}^{Bt}, and $(Fe^{3+}/\text{total Fe})^{Bt}$. This multicolinearity seriously obscures the mixing properties of any one component.

Stepwise least-squares regression and stepwise ridge regression analyses, carried out on subsets of the data population, suggest that Ca mixing into iron-magnesium garnet is significantly nonideal even at low X_{grs} ($\Delta W_{Ca}^{Grt} = 12\,550$ J/mol), consistent with most previous results. The effects of Ti, Fe^{3+}, Mn, and Al mixing in biotite are not significant in this study because of the small or constant amounts of these components in the analyzed biotite. The magnitude of Mn-Mg and Mg-Fe nonideality in garnet cannot be determined from any one data set because of the nearly perfect correlation between X_{sps} and $(X_{alm} - X_{prp})$. Instead, an array of paired values is permitted. For example, if W_{MgFe}^{Grt} is near 0 J/mol, $\Delta W_{Mn}^{Grt} = 5500$ J/mol; if $W_{MgFe}^{Grt} = 8000$ J/mol, $\Delta W_{Mn}^{Grt} = 19000$ J/mol. Simultaneous solution of the three data sets tentatively suggests that the larger values for the two interaction parameters may be more realistic.

Regression results allow a number of models that can successfully describe mixing effects in the analyzed garnets. Two end-member models are proposed. The simplest, permitted because of the strong correlation between X_{sps} and most other components, artificially combines all nonideal mixing in both garnet and biotite into a single X_{sps}-dependent parameter. The small magnitude, approximately 5500 J/mol, of this composite interaction parameter emphasizes that the nonideal mixing effects of all components tend to cancel, resulting in an overall behavior that mimics ideality. A more rigorous approach treats Mn, Fe, and Mg mixing in garnet independently, using an independently constrained Mg-Fe mixing model for garnet. For this study, two recently proposed models from the literature were employed. The simplified and the more rigorous garnet mixing models result in alternative calibrations of the garnet-biotite geothermometer that yield consistent and reasonable temperatures for garnet with X_{sps} between 0 and 0.5.

Introduction

Garnet has complex nonideal solution properties. Mn and Ca apparently do not mix ideally with Fe and Mg, and Fe-Mg mixing itself may not be ideal (Sen and Chakraborty, 1968; Hodges and Spear, 1982; Ganguly and Saxena, 1984; Geiger et al., 1987; Hackler and Wood, 1989). Numerical expressions representing departures from ideality are not well constrained, especially for Mn mixing. These problems limit garnet thermobarometry, including garnet-biotite geothermometry, to rocks low in Mn and Ca.

This study was undertaken to evaluate the mixing properties of Fe-Mg-Mn garnet with the goal of deriving a garnet-biotite geothermometer applicable to Mn-rich rocks. It is based on 77 garnet-biotite specimens collected from the Proterozoic rocks of north-central New Mexico. Although these specimens generally have $X_{grs} < 0.10$, they have X_{sps} ranging from 0 to 0.75.

For this report, suites of 18–30 specimens each were selected from three small areas (Fig. 1): (1) west of Pecos Baldy in the Truchas Range, a region of 1 km^2 where peak metamorphic conditions were near 500 °C, 4 kbar (Grambling, 1986; Grambling et al., 1989); (2) the Rio

0003–004X/90/0708–0886$02.00

Mora uplift, an area of 10 km^2 straddling the kyanite-sillimanite isograd, where peak conditions were near 550 °C, 4.5 kbar (Grambling and Williams, 1985; Grambling et al., 1989); and (3) Cerro Colorado, an area of 1 km^2 in the southern Tusas Mountains, where peak metamorphic conditions were 550–600 °C, 4–5 kbar (Williams, 1987).

Because of the small size of each area, as well as the *P-T* constraints cited in the references above, we have assumed that peak metamorphic conditions were constant within each study area. Most specimens contain staurolite or aluminum silicate, and as a result, most biotites are saturated in the aluminum-biotite component. Chemical variation in garnet and biotite is mainly limited to the Fe^{2+}, Fe^{3+}, Mg, and Mn components.

Analytical techniques

Microprobe analyses were obtained with a JEOL 733 electron microprobe at the Department of Geology, University of New Mexico, using a consistent set of silicate and oxide standards. Operating conditions were 15 kV, 20 nA, with a beam diameter of 1 μm for garnet, 3–10 μm for biotite, and 2–10 μm for Fe-Ti oxides. Coexisting garnet, biotite, and Fe-Ti oxide were analyzed during the same operating session. We examined analytical precision by standard statistical methods and also by reanalyzing selected specimens several months after the original analysis. Precision was better than ± 0.2 wt% for all major elements, and ± 1% of the amount present for elements less abundant than 5 wt%.

Zoned garnets were analyzed by multiple microprobe traverses with step increments less than 10 μm. Detailed two-dimensional maps of garnet zoning were constructed from several samples. Numerous biotite grains were analyzed in each specimen; over 20 and up to 50 spot analyses were obtained from biotite in each thin section.

Fe^{3+}/Fe^{2+} ratios of Fe-Ti oxides were determined by recalculation from microprobe analyses following the method of Rumble (1973). Fe^{3+}/Fe^{2+} ratios of garnet and biotite separates were determined on six samples by Mössbauer spectroscopy by M. Darby Dyar and Roger Burns at the Massachusetts Institute of Technology. Splits from each of the biotite separates, along with five additional biotite separates, were analyzed by wet chemistry at the University of New Mexico. In most cases where both methods were used on the same specimen, Mössbauer spectroscopy and wet-chemical analysis gave similar results. For the few exceptions, Mössbauer data were accepted in preference to wet-chemical data on the assumption that local patches of alteration or fine mineral inclusions, observed in some biotites, biased the wet-chemical results.

Data

Garnet

Garnet typically preserved compositional zoning characterized by continuous declines in X_{sps} and consistent changes in X_{grs} and $X_{alm}/(X_{alm} + X_{prp})$ from cores to points near garnet rims. However, the outermost 5 to 50 μm of many grains showed sharp reversals in the zoning trends, particularly for X_{sps}, X_{alm}, and X_{prp} (see Grambling et al., 1989, Figs. 10 and 11). The thicknesses and magnitudes of these reversals varied even along the rims of single euhedral garnets. Typically, reverse-zoned rims were thickest and most pronounced where garnet was in direct contact with biotite or chlorite. Rims were absent or least pronounced where garnet directly contacted quartz or feldspar. Based on these observations, we have interpreted the reverse zoning as a retrograde feature. For this study, garnet compositions were taken from the edges of traverses not showing the apparent retrograde rims, or at the point of reversal along the zoning profile, with analyses accepted only from samples where the volume of retrograde garnet was insignificant with respect to the volume of biotite. These constraints resulted in compositions that were constant for all garnets in a thin section or even a small outcrop.

It should be noted that the correctness of the interpretation that the zoning reversals are retrograde is not critical to our conclusions. Regardless of the interpretation, the reversals provide a consistent point of comparison for the garnets within a single data set, characterized by a consistent phase assemblage.

Mössbauer analyses showed that 95% of the Fe in garnet is Fe^{2+}. For this study, all Fe was treated as Fe^{2+}. The compositions of 29 low-calcium garnets from Pecos Baldy are in Table 1. X_{sps} varies from 0.00 to 0.32. In 35 specimens collected at Rio Mora, X_{sps} varies from 0.00 to 0.75 (Table 2). From Cerro Colorado, X_{sps} in low-calcium garnets range from 0.01 to 0.47 (Table 3).

Biotite

Biotite is fresh in most samples, but grains in some rocks showed evidence of retrograde or deuteric alteration. The partial alteration included thin streaks of low-interference color parallel to (001), rare stripes of chlorite parallel to (001), and less commonly, small patches of extremely fine-grained chlorite, clay minerals, or epidote. Special care was taken to avoid partial alteration. All optically fresh biotite grains in a thin section varied by less than 1 wt% in all analyzed elements. However, partially altered grains showed variations in K_2O and total weight percent that corresponded to systematic changes in FeO and MgO. Analyses of some altered biotite had no K_2O and gave analytical totals approaching 89 wt%, suggesting that small amounts of clay or chlorite were mixed with the altered biotite.

Microprobe analyses accepted for this study were obtained by analyzing at least 20 optically fresh grains in a single thin section, then averaging the ten analyses with highest K_2O and total weight percent. This technique dramatically reduced the scatter in biotite analyses from a single section. Biotite compositions from the three study areas, screened using these criteria, are in Tables 4, 5, and 6.

Biotite from Cerro Colorado shows somewhat more extensive compositional variation, even within a single

TABLE 1. Microprobe analyses of garnet, Pecos Baldy, New Mexico

	77-85B	76-420	77-125	77-15	77-81E	77-103	76-400B	77-41	76-446	77-39
Weight percent*										
FeO	39.97	39.28	37.24	39.23	39.05	39.92	35.77	38.15	38.43	38.20
MgO	1.75	2.14	2.07	1.51	1.94	1.55	2.08	1.93	1.98	1.88
MnO	0.13	0.14	0.43	0.47	0.60	0.69	0.84	0.88	1.00	1.15
CaO	1.14	0.86	2.21	1.51	1.19	0.91	2.16	1.87	1.88	1.50
TiO_2	0.03	0.02	0.00	0.00	0.04	0.03	0.01	0.03	0.01	0.01
Al_2O_3	21.00	20.69	20.75	20.37	21.08	20.74	20.67	20.78	20.90	20.83
SiO_2	37.41	36.75	37.19	36.75	37.97	37.28	37.02	37.45	37.08	37.01
Total	101.43	99.88	99.89	99.84	101.87	101.12	98.55	101.09	101.28	100.58
Cations**										
Fe	2.686	2.678	2.525	2.686	2.602	2.697	2.448	2.566	2.587	2.587
Mg	0.210	0.260	0.250	0.184	0.230	0.187	0.254	0.231	0.238	0.227
Mn	0.009	0.010	0.030	0.033	0.040	0.047	0.058	0.060	0.068	0.079
Ca	0.098	0.075	0.192	0.132	0.102	0.079	0.189	0.161	0.162	0.130
Ti	0.002	0.001	0.000	0.000	0.002	0.002	0.001	0.002	0.001	0.001
Al	1.989	1.988	1.983	1.965	1.980	1.975	1.994	1.970	1.983	1.988
Si	3.006	2.996	3.015	3.008	3.026	3.012	3.030	3.012	2.985	2.997
Mole fractions†										
alm	0.894	0.886	0.843	0.885	0.875	0.896	0.830	0.850	0.847	0.856
prp	0.070	0.086	0.083	0.061	0.077	0.062	0.086	0.077	0.078	0.075
sps	0.003	0.003	0.010	0.011	0.013	0.016	0.020	0.020	0.022	0.026
grs	0.033	0.025	0.064	0.043	0.034	0.026	0.064	0.053	0.053	0.043

	77-6	77-42	76-445	78-22A	77-73	77-23	83-45	77-46D	84-1632	84-1631
Weight percent*										
FeO	38.94	37.66	39.47	38.24	36.26	37.00	35.25	28.26	28.35	28.67
MgO	1.86	1.86	1.40	1.32	2.02	0.95	1.52	2.94	2.98	3.10
MnO	1.29	1.83	2.34	3.51	3.54	3.80	4.51	8.69	8.96	9.20
CaO	1.49	1.74	0.42	0.34	0.88	1.15	1.09	1.79	1.86	1.66
TiO_2	0.05	0.00	0.01	0.00	0.03	0.01	0.01	0.01	0.04	0.00
Al_2O_3	20.74	20.95	20.94	20.94	21.16	21.08	20.37	21.03	20.78	20.80
SiO_2	37.13	37.11	38.43	36.98	37.52	36.54	36.59	37.64	37.06	37.37
Total	101.50	101.15	103.01	101.33	101.41	100.53	99.34	100.36	100.03	100.80
Cations**										
Fe	2.622	2.538	2.616	2.588	2.430	2.523	2.424	1.894	1.914	1.922
Mg	0.223	0.223	0.165	0.159	0.241	0.115	0.186	0.351	0.359	0.370
Mn	0.088	0.125	0.157	0.241	0.240	0.262	0.314	0.590	0.613	0.625
Ca	0.129	0.150	0.036	0.029	0.076	0.100	0.096	0.154	0.161	0.143
Ti	0.003	0.000	0.001	0.000	0.002	0.001	0.001	0.001	0.002	0.000
Al	1.968	1.989	1.956	1.997	1.998	2.026	1.974	1.986	1.977	1.965
Si	2.990	2.990	3.046	2.993	3.006	2.979	3.009	3.016	2.992	2.996
Mole fractions†										
alm	0.856	0.836	0.880	0.858	0.814	0.841	0.803	0.634	0.628	0.628
prp	0.073	0.073	0.055	0.053	0.081	0.038	0.062	0.117	0.118	0.121
sps	0.029	0.041	0.053	0.080	0.080	0.087	0.104	0.197	0.201	0.204
grs	0.042	0.049	0.012	0.010	0.025	0.033	0.032	0.052	0.053	0.047

	84-1692	76-437	84-169A	76-400	78-25	76-379	77-45	84-1622	84-1621
Weight percent*									
FeO	27.96	30.20	26.97	26.58	26.34	25.76	25.32	21.44	21.77
MgO	2.91	1.44	2.85	2.92	2.90	2.98	2.83	3.03	3.32
MnO	9.32	9.29	9.88	10.52	11.04	11.57	11.73	14.03	14.51
CaO	2.22	1.47	2.13	1.91	2.00	1.85	2.18	3.29	2.79
TiO_2	0.07	0.01	0.00	0.03	0.03	0.02	0.02	0.05	0.08
Al_2O_3	20.90	20.73	21.21	21.01	21.09	21.07	20.81	21.25	21.00
SiO_2	37.06	36.35	36.93	37.99	38.36	37.94	37.91	37.98	37.89
Total	100.44	99.49	99.97	100.96	101.76	101.19	100.80	101.07	101.36
Cations**									
Fe	1.881	2.073	1.819	1.770	1.740	1.713	1.691	1.421	1.442
Mg	0.349	0.176	0.343	0.347	0.341	0.353	0.337	0.358	0.392
Mn	0.635	0.646	0.675	0.710	0.739	0.779	0.793	0.942	0.974
Ca	0.191	0.129	0.184	0.163	0.169	0.158	0.186	0.279	0.237
Ti	0.004	0.001	0.000	0.002	0.002	0.001	0.001	0.003	0.005
Al	1.982	2.005	2.016	1.972	1.964	1.974	1.958	1.984	1.961
Si	2.981	2.983	2.978	3.025	3.031	3.017	3.027	3.009	3.002
Mole fractions†									
alm	0.616	0.686	0.602	0.592	0.582	0.570	0.562	0.474	0.474
prp	0.114	0.058	0.114	0.116	0.114	0.118	0.112	0.119	0.129
sps	0.208	0.214	0.223	0.237	0.247	0.259	0.264	0.314	0.320
grs	0.063	0.043	0.061	0.055	0.057	0.053	0.062	0.093	0.078

* Weight percent TiO_2 is below detection in all garnets.
** Based on 12 O atoms.
† alm = cations Fe/cations (Fe + Mg + Mn + Ca).

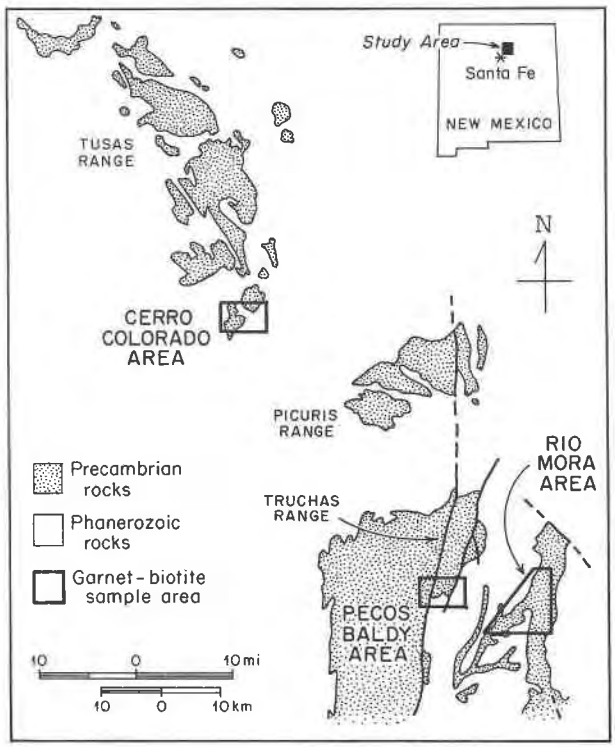

Fig. 1. Generalized geologic map showing exposures of Proterozoic rocks in a part of north-central New Mexico. Boxes outline sampling areas.

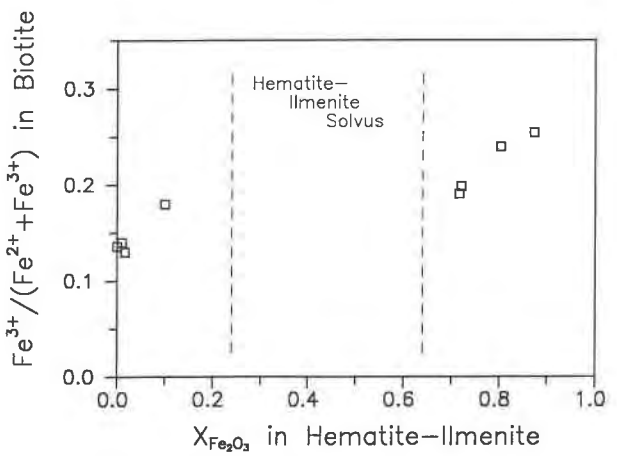

Fig. 2. $Fe^{3+}/(Fe^{3+} + Fe^{2+})$ in biotite plotted against mole fraction of hematite in hematite-ilmenite. Fe^{3+}/Fe^{2+} ratios are from wet-chemical and Mössbauer analyses of biotite separates. Oxides were analyzed with the electron microprobe (Table 7). All samples are from the Rio Mora map area (Table 5).

thin section, than that from the other two study areas. Although we have eliminated all samples with obviously altered biotite, we suspect that the greater scatter observed in these data may reflect greater degrees of retrogression (enhanced by the higher peak temperature) and minor amounts of alteration. This region, unlike the other two, was not recently glaciated.

Fe^{3+} in biotite. The Fe^{3+}/Fe^{2+} ratio of biotite is expected to vary with f_{O_2}, an expectation supported by Figure 2. $Fe^{3+}/(Fe^{3+} + Fe^{2+})$ in biotite, calculated on a cation basis, increases from 0.13 in rocks with $X_{Fe_2O_3}^{Ilm\text{-}Hem} = 0$ to 0.26 in rocks with $X_{Fe_2O_3}^{Ilm\text{-}Hem} = 0.86$, with an expected complication induced by the ilmenite-hematite phase transition. Figure 2 provides a useful way to estimate Fe^{3+} in biotites that have not been analyzed directly for Fe^{3+}. Fe^{3+}/Fe^{2+} ratios, determined directly for eight samples from Rio Mora and estimated using Figure 2 for the remaining samples, are included in Table 5.

Although $Fe^{3+}/(Fe^{3+} + Fe^{2+})$ in biotite increases with $X_{Fe_2O_3}^{Ilm\text{-}Hem}$ (i.e., with f_{O_2}), the absolute number of Fe^{3+} cations in biotite varies little, decreasing slightly as f_{O_2} increases. Calculated on the basis of 11 O per formula unit, biotite has 0.20 cations Fe^{3+} at relatively low f_{O_2} but only 0.12 cations Fe^{3+} in samples with hematite. This is not as anomalous as it might seem, because total Fe in biotite falls sharply as f_{O_2} increases. Such behavior is consistent with wet-chemical data presented in previous studies (Chinner, 1960; Phinney, 1963; Hounslow and Moore, 1967).

For this study, mole fractions for octahedral cations in biotite were calculated using two techniques. The first assigned Al cations to all tetrahedral sites not occupied by Si. The remaining Al and all Fe, Fe^{3+}, Ti, Mg, and Mn were assumed to be in octahedral sites. The second technique assumed that some Fe^{3+} was tetrahedrally coordinated in biotite (as suggested by M. Darby Dyer, personal communication). In all samples, Fe^{3+} exceeded 10% of total Fe. Therefore, for the purpose of comparison, we assumed that 10% of the total Fe was tetrahedrally coordinated. Vacant tetrahedral sites were then assumed to be filled with Al and all remaining cations were considered to be in octahedral sites. These two techniques resulted in two distinct values for X_{Al}^{Bt} and $X_{Fe^{3+}}^{Bt}$, and thus may have an effect on regression analyses that investigate mixing of these phase components.

Ilmenite-hematite

Ilmenite and hematite showed some retrograde or supergene alteration. Exsolution lamellae were evident in most grains, and some ilmenite crystals were altered to a mixture of geothite and leucoxene. Altered crystals were avoided during microprobe analysis.

Several techniques were tested to overcome the problem of exsolution. These included (1) averaging numerous broad-beam microprobe analyses from single exsolved grains, (2) determining compositions of subdomains within exsolved crystals and then, using back-scatter electron imaging, calculating the homogenized oxide composition, and (3) measuring compositions of oxides found as small inclusions in other metamorphic minerals. The most consistent and reproducible oxide analyses were obtained from small oxide inclusions (2–30 μm in diameter) found within matrix grains of quartz. These inclusions,

TABLE 2. Microprobe analyses of garnet, Rio Mora, New Mexico

	81-23a	80-142	80-46	80-46b	C81-174	80-30	80-43	80-187	80-42	80-20	80-51	C81-181
Weight percent*												
FeO	39.10	39.19	40.16	39.70	39.63	39.64	39.87	38.01	40.23	39.69	37.39	36.88
MgO	2.51	2.06	2.04	2.00	1.55	2.30	2.20	2.32	2.22	1.72	2.23	3.06
MnO	0.23	0.34	0.43	0.44	0.47	0.53	0.54	0.55	0.61	0.85	0.86	1.23
CaO	1.03	0.45	0.54	0.55	1.75	0.75	0.65	1.32	0.43	0.57	1.58	1.54
TiO_2	0.02	0.00	0.02	0.00	0.02	0.00	0.00	0.04	0.00	0.01	0.00	0.00
Al_2O_3	20.85	20.96	20.96	20.62	20.95	20.91	20.92	21.03	21.05	20.73	20.80	20.90
SiO_2	37.53	36.31	37.27	37.31	37.30	37.62	37.47	37.42	37.88	37.18	37.41	36.05
Total	101.27	99.31	101.42	100.62	101.67	101.75	101.65	100.69	102.42	100.75	100.27	99.66
Cations**												
Fe	2.621	2.688	2.701	2.688	2.662	2.651	2.673	2.557	2.675	2.689	2.525	2.515
Mg	0.300	0.252	0.245	0.241	0.186	0.274	0.263	0.278	0.263	0.208	0.268	0.372
Mn	0.016	0.024	0.029	0.030	0.032	0.036	0.037	0.037	0.041	0.058	0.059	0.085
Ca	0.088	0.040	0.047	0.048	0.151	0.064	0.056	0.114	0.037	0.049	0.137	0.135
Ti	0.001	0.000	0.001	0.000	0.001	0.000	0.000	0.002	0.000	0.001	0.000	0.000
Al	1.970	2.026	1.987	1.968	1.983	1.971	1.976	1.993	1.973	1.980	1.980	2.009
Si	3.009	2.978	2.998	3.021	2.996	3.009	3.004	3.010	3.012	3.012	3.021	2.940
Mole fractions†												
alm	0.866	0.895	0.894	0.894	0.878	0.876	0.882	0.856	0.887	0.895	0.845	0.809
prp	0.099	0.084	0.081	0.080	0.061	0.091	0.087	0.093	0.087	0.069	0.090	0.120
sps	0.005	0.008	0.010	0.010	0.011	0.012	0.012	0.012	0.014	0.019	0.020	0.027
grs	0.029	0.013	0.016	0.016	0.050	0.021	0.018	0.038	0.012	0.016	0.046	0.043

	80-178a	81-225	80-18a	80-192-2	81-234	C81-148	C81-105	C81-213	81-13a	C81-310	80-178	81-145
Weight percent*												
FeO	37.11	31.64	36.06	35.55	30.72	34.82	32.65	27.41	25.25	26.57	26.49	20.15
MgO	2.36	5.70	2.30	2.33	4.59	2.32	1.87	3.29	2.76	3.35	2.96	5.48
MnO	1.62	1.73	1.67	1.87	3.00	4.06	5.40	10.23	10.52	10.68	10.58	12.43
CaO	1.07	2.42	2.05	2.59	2.14	1.81	2.93	1.67	3.64	1.44	1.73	3.40
TiO_2	0.00	0.00	0.01	0.00	0.00	0.02	0.00	0.00	0.04	0.03	0.00	0.03
Al_2O_3	20.95	21.21	20.93	20.90	20.87	20.76	20.36	20.97	20.63	21.05	21.00	21.07
SiO_2	37.80	37.49	37.39	37.54	38.23	36.38	36.86	37.48	37.19	37.62	37.24	38.55
Total	100.91	100.19	100.41	100.78	99.55	100.17	100.07	101.05	100.03	100.74	100.00	101.11
Cations**												
Fe	2.488	2.096	2.429	2.385	2.045	2.370	2.221	1.830	1.701	1.774	1.784	1.317
Mg	0.282	0.673	0.276	0.279	0.545	0.281	0.227	0.391	0.331	0.399	0.355	0.638
Mn	0.110	0.116	0.114	0.127	0.202	0.280	0.372	0.692	0.718	0.722	0.722	0.823
Ca	0.092	0.205	0.177	0.223	0.183	0.158	0.255	0.143	0.314	0.123	0.149	0.285
Ti	0.000	0.000	0.001	0.000	0.000	0.001	0.000	0.000	0.002	0.002	0.000	0.002
Al	1.979	1.980	1.987	1.976	1.958	1.991	1.952	1.973	1.959	1.981	1.994	1.940
Si	3.030	2.970	3.011	3.011	3.044	2.961	2.998	2.992	2.996	3.004	2.999	3.012
Mole fractions†												
alm	0.837	0.678	0.811	0.791	0.687	0.767	0.722	0.599	0.555	0.588	0.593	0.430
prp	0.095	0.218	0.092	0.093	0.183	0.091	0.074	0.128	0.108	0.132	0.118	0.208
sps	0.037	0.038	0.038	0.042	0.068	0.091	0.121	0.226	0.234	0.239	0.240	0.269
grs	0.031	0.066	0.059	0.074	0.062	0.051	0.083	0.047	0.102	0.041	0.050	0.093

						High-Mn garnets, excluded from regression analysis					
	81-70a	80-218	82-62	C81-244	82-12	84-147e	84-147d	81-221	81-175a	81-139	81-139a
Weight percent*											
FeO	25.60	22.46	17.17	17.58	16.83	9.51	9.98	5.45	1.61	0.66	0.55
MgO	3.31	3.66	4.22	4.13	4.77	4.42	4.06	1.96	3.12	4.11	4.14
MnO	12.26	14.38	17.31	18.35	18.72	22.97	22.94	28.79	32.22	33.68	34.06
CaO	1.14	1.70	2.89	1.61	1.47	4.00	3.34	5.67	4.23	2.49	2.43
TiO_2	0.03	0.08	0.03	0.09	0.03	0.04	0.04	0.04	0.05	0.08	0.02
Al_2O_3	20.97	20.89	21.09	20.45	21.15	21.08	21.12	20.26	20.70	20.76	21.10
SiO_2	37.63	37.88	38.07	37.49	37.94	37.71	38.49	37.06	37.49	36.93	37.54
Total	100.94	101.05	100.78	99.70	100.91	99.73	99.97	99.23	99.42	98.71	99.84
Cations**											
Fe	1.709	1.492	1.135	1.181	1.112	0.632	0.660	0.370	0.108	0.045	0.037
Mg	0.394	0.433	0.497	0.494	0.562	0.523	0.478	0.237	0.373	0.495	0.492
Mn	0.829	0.968	1.158	1.248	1.252	1.546	1.536	1.978	2.191	2.304	2.300
Ca	0.098	0.145	0.245	0.139	0.124	0.341	0.283	0.493	0.364	0.216	0.208
Ti	0.002	0.005	0.002	0.005	0.002	0.002	0.002	0.002	0.003	0.005	0.001
Al	1.973	1.956	1.964	1.936	1.969	1.974	1.968	1.937	1.959	1.976	1.983
Si	3.004	3.009	3.008	3.011	2.997	2.996	3.043	3.006	3.010	2.983	2.993
Mole fractions†											
alm	0.564	0.491	0.374	0.386	0.365	0.208	0.223	0.120	0.036	0.015	0.012
prp	0.130	0.143	0.164	0.161	0.184	0.172	0.162	0.077	0.123	0.162	0.162
sps	0.274	0.319	0.382	0.408	0.410	0.508	0.519	0.643	0.722	0.753	0.757
grs	0.032	0.048	0.081	0.045	0.041	0.112	0.096	0.160	0.120	0.071	0.068

* Weight percent TiO_2 is below detection in all garnets.
** Based on 12 O atoms.
† alm = cations Fe/cations (Fe + Mg + Mn + Ca).

which typically lacked exsolution textures, were interpreted to have been trapped as quartz annealed near the peak of metamorphism and were accepted as oxide compositions at peak metamorphic conditions. The armoring quartz may have protected the inclusions from subsequent retrograde or deuteric alteration. Typically, at least some larger matrix oxide grains have compositions identical to the small inclusions. Table 7 presents analyses of peak oxide minerals.

Thermodynamic expressions

The systematics of Fe-Mg partitioning between garnet and biotite have been presented by Ganguly and Kennedy (1974), and Ganguly and Saxena (1984), and Ganguly and Saxena (1987). The Fe-Mg exchange reaction can be expressed as

$$\underset{\text{almandine}}{\tfrac{1}{3}Fe_3Al_2Si_3O_{12}} + \underset{\text{phlogopite}}{\tfrac{1}{3}KMg_3AlSi_3O_{10}(OH)_2} = \underset{\text{pyrope}}{\tfrac{1}{3}Mg_3Al_2Si_3O_{12}} + \underset{\text{annite}}{\tfrac{1}{3}KFe_3AlSi_3O_{10}(OH)_2}. \quad (1)$$

At equilibrium

$$K_{eq} = \frac{(X_{prp}/X_{alm})}{(X_{Mg}/X_{Fe})^{Bt}} \times \frac{(\gamma_{prp}/\gamma_{alm})}{(\gamma_{Mg}/\gamma_{Fe})^{Bt}} \quad (2)$$

where the first term (K_{eq}) is the equilibrium constant for Equation 1, the second, compositional, term (K_D) is the distribution coefficient, and the third term (K_γ) treats nonideal mixing.

Following Ganguly and Saxena (1984, 1987), we assume that mixing in garnet and biotite can be approximated by a simple mixture model (Guggenheim, 1967) within the compositional range of our isothermal-isobaric suites of samples, and we ignore multicomponent interactions. With these assumptions, Equation 2 can be rewritten as

$$\begin{aligned} -RT \ln K_D = &-RT \ln K_{eq} \\ &+ [W_{MgFe}(X_{alm} - X_{prp}) + \Delta W_{Ca}(X_{grs}) \\ &\quad + \Delta W_{Mn}(X_{sps})]^{Grt} \\ &- [W_{MgFe}(X_{Fe} - X_{Mg}) - \Delta W_{Mn}(X_{Mn}) \\ &\quad - \Delta W_{Ti}(X_{Ti}) - \Delta W_{Al}(X_{Al}) \\ &\quad - \Delta W_{Fe^{3+}}(XFe^{3+})]^{Bt} \end{aligned} \quad (3)$$

where W_{ij} represents a binary simple mixture interaction parameter and $\Delta W_i = (W_{iMg} - W_{iFe})$. All biotite mixing terms refer exclusively to cations in octahedral sites. The $W_{i,j}$ terms can be modeled as constant over a limited compositional range (symmetric mixing) or as a variable function of composition (asymmetric mixing). Equation 3 assumes that, along with Fe and Mg, the octahedral substituents in biotite are Mn, Fe^{3+}, Al, and Ti and the eightfold substituents in garnet are Mn and Ca.

Constraints on garnet and biotite mixing parameters

Garnet. Most early investigators assumed that Mg-Fe mixing in garnet is nearly ideal, and Ferry and Spear (1978) found no evidence in their experiments for nonideality. However, based on an analysis of experimental and natural data, Ganguly and Saxena (1984) suggested that Mg-Fe mixing is significantly nonideal and that nonideality is asymmetric, reaching a maximum in Fe-rich garnets. This suggestion has been supported by experimental data (Geiger et al., 1987). Ganguly and Saxena (1984) proposed a symmetric approximation for asymmetric Mg-Fe mixing where

$$\begin{aligned} W^{Grt}_{MgFe} = &W_{Fe\text{-}Mg}[X_{prp}/(X_{prp} + X_{alm})] \\ &+ W_{Mg\text{-}Fe}[X_{alm}/(X_{prp} + X_{alm})] \end{aligned} \quad (4)$$

with $W_{Mg\text{-}Fe} = 10460$ J/mol and $W_{Fe\text{-}Mg} = 835$ J/mol (one-site basis). Recently, Hackler and Wood (1989) concluded that this model is incompatible with experimental partitioning data, especially at high X_{alm}. Using the new and existing experimental data, they concluded that Mg-Fe mixing behavior is much more nearly ideal, $W_{Mg\text{-}Fe} = 2100$ J/mol and $W_{Fe\text{-}Mg} = 700$ J/mol.

Most workers have agreed that Ca does not mix ideally in magnesium-iron garnet (cf. Hodges and Spear, 1982; Ganguly and Saxena, 1984; Hodges and Crowley, 1985; Anovitz and Essene, 1987; Geiger et al., 1987). Ganguly and Saxena suggest a value of 12550 J/mol for ΔW_{Ca} for X_{grs} below 0.10, a value supported by the experiments of Geiger et al. (1987).

Ganguly and Kennedy (1974) suggest that Mn-Fe mixing is nearly ideal in garnet, but Mn-Mg mixing may be significantly nonideal (Ganguly and Kennedy, 1974; Ganguly and Saxena, 1984). Using partitioning of Mn between garnet and ilmenite, O'Neill et al. (1989) concluded that W_{MnFe} is approximately 1800 J/mol, but until present, W_{MnMg} has been largely unconstrained. Many workers have observed a negative correlation between X_{sps} and $K_D^{Bt\text{-}Grt}$ (Ganguly and Kennedy, 1974; Dahl, 1980; Newton and Haselton, 1981; St. Onge, 1984; and this study), and using regression analyses of natural data, Ganguly and Saxena (1984) proposed that ΔW_{Mn} is approximately 12550 J/mol. However, as discussed below, the negative correlation may result from multicolinearity in the compositional data and thus may not directly constrain Mn mixing behavior.

Biotite. Following Mueller (1972), most workers have assumed that Fe and Mg mix ideally in biotite. There are few data to contradict this assumption, although Ganguly and Saxena (1984, p. 92) allowed that Fe-Mg mixing may show some positive departure from ideality. Nonideal Mn mixing is unlikely to be important in biotite because of its vanishingly small amounts of Mn, even where biotite coexists with spessartitic garnet.

Several other components may mix nonideally in magnesium-iron biotite. Dallmeyer (1974) and Indares and Martignole (1985) have shown that K_D correlates positively with Fe^{3+}, Al, and Ti in biotite. The effects of nonideal mixing of these components are probably most important in the upper amphibolite to granulite facies, where Al and Ti become major substituents. As noted above,

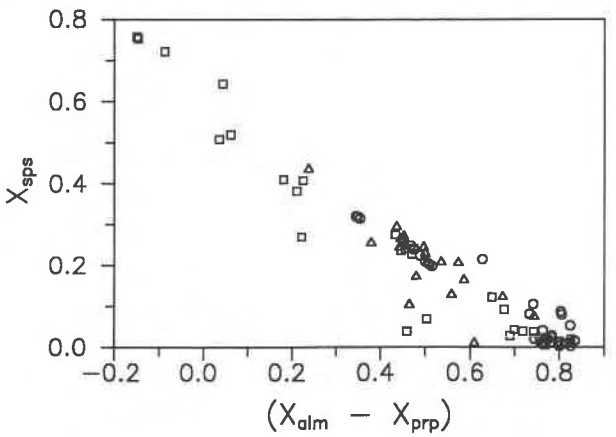

Fig. 3. X_{sps} plotted against $(X_{alm} - X_{prp})$ for garnets from Rio Mora (squares), Pecos Baldy (circles), and Cerro Colorado (triangles), New Mexico (slope = −0.70, x-intercept = 0.77, and r^2 = 0.94).

the mole fraction of the aluminum biotite component is relativley constant in biotite from New Mexico.

Regression analysis

Multicolinearity of compositional variables

For an isothermal-isobaric set of garnet-biotite pairs, such as any one of the three sets presented here, statistical regression of ln K_D against the compositional variables (X_i) in Equation 3 should constrain the values of the binary interaction parameters (Ganguly and Saxena, 1987). However, the results of the regression analysis may be compromised when two or more compositional variables are highly correlated, meaning that at least one variable can be predicted from the others (Devore, 1982; Belsley et al., 1980). Correlation coefficients for the variables in Equation 3, based upon analyses of the New Mexico rocks, are shown in Table 8. Strong correlations exist among many of the variables. Most importantly for Mn-bearing garnets, X_{sps} is correlated to some degree with most other compositional variables, and it is strongly correlated with $(X_{alm} - X_{prp})$ (correlation coefficient >0.9). This last correlation is extremely important because X_{sps} and $(X_{alm} - X_{prp})$ are probably the two most important nonideally mixing components in Equation 3. These correlations have an important effect on the magnitude of the regression coefficients (interaction parameters), and, therefore, on any conclusions about garnet mixing behavior and the garnet-biotite Fe-Mg exchange equilibrium. One additional correlation, between X_{sps} and f_{O_2}, must also be considered. Several of the strongest linear relationships are discussed individually in the following section.

X_{sps} vs. $(X_{alm} - X_{prp})$. A negative linear correlation between X_{sps} and $(X_{alm} - X_{prp})$ characterizes all 85 analyzed samples (Fig. 3). The correlation coefficient for a linear fit to all data is high (r^2 = 0.91). Separate linear regressions of specimens from each individual study area yield slightly different slopes, −0.64, −0.74, and −0.70 for Pecos Baldy, Rio Mora, and Cerro Colorado, respectively. These slopes are statistically distinct at the 98% confidence level.

This correlation is a consequence of phase equilibrium as shown on an MgO-FeO-MnO projection in Figure 4. For amphibolite-facies samples, all garnets coexisting with staurolite, aluminum silicate, or chlorite must lie along a linear trend nearly parallel to the FeO-MnO side of the triangle. Because lines of constant $(X_{alm} - X_{prp})$ are perpendicular to the MgO-FeO side, Mn and (Fe-Mg) will tend to be negatively correlated. Further, a negative X_{sps} vs. $(X_{alm} - X_{prp})$ correlation would be expected to char-

Table 3. Microprobe analyses of garnet, Cerro Colorado, New Mexico

	W83-302	W84-35	W84-86	W84-94	W84-117	W84-130	W83-300	W84-145
Weight percent*								
FeO	35.50	36.00	28.39	32.64	29.99	30.23	27.07	29.47
MgO	4.24	1.61	4.24	1.66	2.63	2.30	3.08	2.18
MnO	0.58	3.38	4.64	5.45	5.80	7.29	7.71	9.17
CaO	1.75	1.78	3.19	2.33	3.67	2.22	3.58	1.53
Al_2O_3	20.69	20.78	20.64	20.69	20.98	20.73	21.07	20.79
SiO_2	36.72	37.21	37.40	36.96	37.60	37.33	37.23	37.38
Total	99.48	100.76	98.50	99.73	100.67	100.10	99.74	100.52
Cations**								
Fe	2.400	2.433	1.915	2.222	2.004	2.042	1.819	1.987
Mg	0.511	0.194	0.510	0.201	0.313	0.277	0.369	0.262
Mn	0.040	0.231	0.317	0.376	0.393	0.499	0.525	0.626
Ca	0.152	0.154	0.276	0.203	0.314	0.192	0.308	0.132
Al	1.971	1.980	1.963	1.985	1.976	1.973	1.995	1.976
Si	2.969	3.008	3.017	3.009	3.004	3.015	2.991	3.014
Mole fractions†								
alm	0.773	0.808	0.635	0.740	0.663	0.678	0.602	0.661
prp	0.165	0.064	0.169	0.067	0.104	0.092	0.122	0.087
sps	0.013	0.077	0.105	0.125	0.130	0.166	0.174	0.208
grs	0.049	0.051	0.091	0.068	0.104	0.064	0.102	0.044

* Weight percent TiO_2 is below detection in all garnets.
** Based on 12 O atoms.
† alm = cations Fe/cations (Fe + Mg + Mn + Ca).

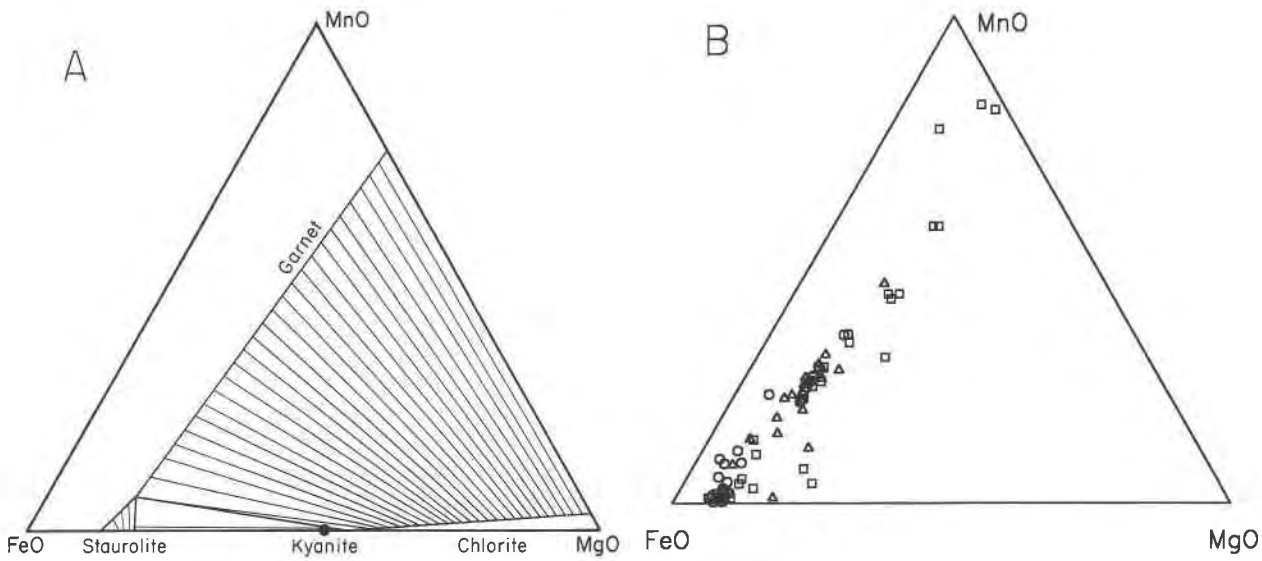

Fig. 4. (**A**) Generalized FeO-MgO-MnO projection from quartz, muscovite, H_2O, and biotite (modified after Spear, 1988). (**B**) FeO-MgO-MnO plot for samples from Rio Mora (squares), Pecos Baldy (circles), and Cerro Colorado (triangles), New Mexico. Following Spear (1988), molar FeO-MgO-MnO ratios of the garnets have been plotted. Note that lines of constant (FeO-MgO) are perpendicular to the FeO-MgO side of the triangle. Thus, for staurolite-, chlorite-, or aluminum-silicate-bearing samples, a linear relationship between X_{sps} and $(X_{alm} - X_{prp})$ is predicted.

acterize pelitic garnet-bearing assemblages elsewhere. Figure 5 illustrates this based on the garnet- and staurolite-zone samples analyzed by Ferry (1980). Similar correlations can be seen in most other compilations of garnet analyses (cf. Phinney, 1963; Hodges and Spear, 1982; Hudson, 1985). A consequence of this correlation is that all garnet specimens reported in Tables 1–3, that have $(X_{sps} + X_{grs})$ less than 0.04, have nearly identical X_{alm}, 0.89 $\pm$ 0.02, regardless of the specific assemblage in which they occur. The same X_{alm} is derived by projecting Ferry's (1980) garnet analyses (Fig. 5) to $X_{sps} = 0$. This helps to explain the widespread success of the Ferry and Spear (1978) garnet-biotite calibration applied to garnets low in Mn and Ca: their experiments were carried out on garnet of virtually the same X_{alm} as those most common in nature.

A similar negative linear correlation couples X_{sps} to $(X_{Fe} - X_{Mg})^{Bt}$ or $(X_{Fe}/X_{Mg})^{Bt}$. This is required by chemical equi-

Table 3.—*Continued*

W85-195	W84-58	W84-153	W84-87	W85-253	W84-75	W83-242	W84-133	W85-254
28.21	27.03	25.51	26.41	23.49	25.74	25.03	24.62	17.27
2.37	2.63	3.23	2.50	3.69	3.11	2.74	2.87	3.68
9.27	10.18	10.80	10.74	11.35	11.90	11.97	13.04	19.58
2.25	2.05	1.83	1.88	2.37	1.53	1.90	1.35	1.23
21.45	20.75	21.06	20.96	20.86	20.83	20.57	20.95	20.90
37.85	37.56	37.77	37.34	38.08	37.18	38.00	36.88	37.76
101.40	100.20	100.20	99.83	99.84	100.29	100.21	99.71	100.42
1.875	1.819	1.706	1.783	1.568	1.733	1.680	1.667	1.153
0.281	0.315	0.385	0.301	0.439	0.373	0.328	0.346	0.438
0.624	0.694	0.732	0.734	0.767	0.811	0.814	0.894	1.324
0.192	0.177	0.157	0.163	0.203	0.132	0.163	0.117	0.105
2.009	1.968	1.985	1.994	1.962	1.976	1.945	1.999	1.966
3.008	3.022	3.021	3.014	3.039	2.992	3.049	2.987	3.014
0.631	0.605	0.572	0.598	0.527	0.568	0.563	0.551	0.382
0.095	0.105	0.129	0.101	0.147	0.122	0.110	0.114	0.145
0.210	0.231	0.246	0.246	0.258	0.266	0.273	0.296	0.438
0.065	0.059	0.053	0.055	0.068	0.043	0.055	0.039	0.035

TABLE 4. Microprobe analyses of biotite, Pecos Baldy, New Mexico

	77-85B	76-420	77-125	77-15	77-81E	77-103	76-400B	77-41	76-446	77-39
Weight percent*										
FeO	23.70	21.55	20.63	24.68	22.75	23.22	19.88	21.38	22.26	21.89
MgO	6.70	7.81	8.50	6.30	7.07	6.21	8.76	8.30	8.50	7.96
MnO	0.00	0.01	0.00	0.00	0.00	0.00	0.00	0.01	0.00	0.00
TiO_2	1.59	1.57	1.50	1.56	1.58	1.48	1.43	1.37	1.46	1.45
Al_2O_3	20.43	20.31	20.44	19.94	20.19	20.56	19.95	20.19	19.97	20.34
SiO_2	34.40	34.49	35.46	33.41	34.16	34.14	33.97	35.44	35.24	34.42
K_2O	8.74	8.91	8.54	8.18	8.62	8.70	8.64	8.34	8.69	8.42
Na_2O	0.32	0.25	0.32	0.16	0.31	0.21	0.33	0.27	0.33	0.35
CaO	0.001	0.060	0.040	0.030	0.040	0.020	0.000	0.020	0.030	0.007
Total	95.88	94.96	95.43	94.26	94.72	94.54	92.96	95.32	96.48	94.84
% Fe^{3+}	0.12	0.13	0.14	0.12	0.13	0.12	0.15	0.13	0.14	0.13
Cations**										
Fe^{2+}	1.331	1.197	1.116	1.416	1.273	1.319	1.094	1.175	1.202	1.216
Fe^{3+}	0.181	0.179	0.182	0.193	0.190	0.180	0.193	0.176	0.196	0.182
Mg	0.762	0.889	0.953	0.732	0.810	0.715	1.011	0.934	0.952	0.906
Mn	0.000	0.001	0.000	0.000	0.000	0.000	0.000	0.001	0.000	0.000
Ti	0.091	0.090	0.085	0.091	0.091	0.086	0.083	0.078	0.082	0.083
Al	1.837	1.828	1.812	1.832	1.830	1.871	1.820	1.797	1.768	1.831
Si	2.624	2.633	2.667	2.605	2.627	2.636	2.629	2.676	2.647	2.628
K	0.851	0.868	0.819	0.814	0.846	0.857	0.853	0.803	0.833	0.820
Na	0.047	0.037	0.047	0.024	0.046	0.031	0.050	0.040	0.048	0.052
Ca	0.000	0.005	0.003	0.003	0.003	0.002	0.000	0.002	0.002	0.001

	77-6	77-42	76-445	78-22A	77-73	77-23	83-45	77-46D	84-1632	84-1631
Weight percent*										
FeO	23.11	22.86	25.09	24.85	21.88	26.66	22.46	16.29	16.68	16.60
MgO	7.10	7.95	6.34	5.94	8.86	5.12	7.42	12.15	12.62	12.73
MnO	0.00	0.01	0.01	0.04	0.00	0.06	0.05	0.10	0.15	0.14
TiO_2	1.58	1.45	1.45	1.48	1.63	1.69	1.60	1.37	1.34	1.34
Al_2O_3	20.32	20.65	21.34	20.55	20.13	20.49	20.09	19.47	19.45	19.67
SiO_2	34.15	34.92	34.06	33.91	34.95	33.89	34.94	36.21	35.91	36.20
K_2O	9.27	8.55	8.91	8.84	7.82	7.38	8.80	9.05	9.19	9.28
Na_2O	0.19	0.33	0.11	0.18	0.17	0.18	0.10	0.43	0.49	0.47
CaO	0.040	0.025	0.000	0.016	0.060	0.050	0.003	0.015	0.000	0.000
Total	95.76	96.75	97.31	95.80	95.50	95.52	95.46	95.09	95.83	96.43
% Fe^{3+}	0.13	0.13	0.13	0.12	0.14	0.16	0.14	0.19	0.21	0.21
Cations**										
Fe^{2+}	1.286	1.249	1.379	1.406	1.186	1.438	1.228	0.819	0.814	0.804
Fe^{3+}	0.192	0.186	0.206	0.191	0.193	0.273	0.200	0.192	0.216	0.214
Mg	0.809	0.889	0.714	0.680	0.995	0.586	0.841	1.344	1.390	1.392
Mn	0.000	0.001	0.001	0.003	0.000	0.004	0.003	0.006	0.009	0.009
Ti	0.091	0.082	0.082	0.086	0.092	0.098	0.091	0.076	0.074	0.074
Al	1.831	1.827	1.900	1.862	1.788	1.855	1.800	1.703	1.693	1.700
Si	2.611	2.621	2.573	2.606	2.634	2.603	2.656	2.687	2.653	2.655
K	0.904	0.819	0.859	0.867	0.752	0.723	0.853	0.857	0.866	0.868
Na	0.028	0.048	0.016	0.027	0.025	0.027	0.015	0.062	0.070	0.067
Ca	0.003	0.002	0.000	0.001	0.005	0.004	0.000	0.001	0.000	0.000

	84-1692	76-437	84-169A	76-400	78-25	76-379	77-45	84-1622	84-1621
Weight percent*									
FeO	16.29	21.59	16.55	15.59	15.65	14.58	15.16	12.72	12.75
MgO	12.79	7.91	12.60	12.60	12.23	13.48	12.42	14.91	15.64
MnO	0.14	0.16	0.12	0.15	0.18	0.17	0.13	0.15	0.20
TiO_2	1.32	1.81	1.36	1.35	1.41	1.36	1.42	1.19	1.04
Al_2O_3	19.59	19.13	19.13	19.41	19.43	19.21	19.22	18.80	18.47
SiO_2	35.95	34.28	36.87	36.32	37.06	36.94	36.10	37.44	37.39
K_2O	9.22	8.76	9.07	8.91	8.65	9.06	9.09	9.10	9.15
Na_2O	0.40	0.18	0.44	0.45	0.52	0.45	0.43	0.35	0.30
CaO	0.005	0.005	0.002	0.002	0.000	0.000	0.009	0.000	0.000
Total	95.71	93.83	96.14	94.78	95.13	95.25	93.97	94.66	94.94
% Fe^{3+}	0.22	0.12	0.22	0.20	0.22	0.20	0.22	0.25	0.25
Cations**									
Fe^{2+}	0.784	1.231	0.791	0.773	0.751	0.716	0.739	0.584	0.584
Fe^{3+}	0.221	0.168	0.223	0.193	0.211	0.179	0.208	0.194	0.195
Mg	1.406	0.914	1.377	1.393	1.341	1.476	1.383	1.626	1.703
Mn	0.009	0.011	0.007	0.009	0.011	0.011	0.008	0.009	0.012
Ti	0.073	0.105	0.075	0.075	0.078	0.075	0.080	0.065	0.057
Al	1.703	1.747	1.653	1.696	1.685	1.663	1.693	1.621	1.590
Si	2.652	2.657	2.703	2.693	2.727	2.714	2.697	2.739	2.731
K	0.868	0.866	0.848	0.843	0.812	0.849	0.866	0.849	0.853
Na	0.057	0.027	0.063	0.065	0.074	0.064	0.062	0.050	0.042
Ca	0.000	0.000	0.000	0.000	0.000	0.000	0.001	0.000	0.000

* % $Fe^{3+} = Fe^{3+}/(Fe^{3+} + Fe^{2+})$, estimated based on composition of coexisting oxides and Figure 3.
** Based on 11 O atoms.

TABLE 5. Microprobe analyses of biotite, Rio Mora, New Mexico

Sample	81-23a	80-142*	80-46*	80-46b	C81-174	80-30*	80-43	80-187	80-42	80-20	80-51	C81-181
Weight percent*												
FeO	21.66	23.12	23.27	23.06	25.05	22.77	23.75	20.94	23.30	24.92	21.47	20.78
MgO	8.24	6.25	6.89	6.66	6.13	7.29	6.85	8.30	6.71	5.63	8.05	9.71
MnO	0.00	0.00	0.00	0.01	0.00	0.01	0.00	0.00	0.00	0.00	0.00	0.00
TiO_2	1.62	2.08	1.91	2.00	2.03	2.25	1.98	1.75	1.84	2.10	1.76	1.55
Al_2O_3	20.54	20.37	20.29	20.40	19.65	20.37	20.35	20.34	20.47	20.14	20.17	19.29
SiO_2	34.99	33.87	34.25	34.43	34.16	33.43	34.31	35.02	34.46	33.86	34.66	35.02
K_2O	8.66	9.08	8.96	8.69	9.22	8.99	9.03	8.93	9.13	8.91	9.06	9.06
Na_2O	0.42	0.36	0.34	0.31	0.21	0.23	0.30	0.29	0.15	0.42	0.36	0.17
CaO	0.02	0.00	0.00	0.00	0.01	0.00	0.00	0.00	0.00	0.01	0.00	0.00
Total	96.15	95.13	95.91	95.56	96.46	95.34	96.57	95.57	96.06	95.99	95.53	95.58
% Fe^{3+}	0.14	0.14	0.13	0.12	0.12	0.13	0.12	0.13	0.12	0.13	0.15	0.15
Cations**												
Fe^{2+}	1.17	1.28	1.29	1.30	1.41	1.27	1.33	1.15	1.31	1.39	1.16	1.12
Fe^{3+}	0.19	0.21	0.19	0.18	0.19	0.19	0.18	0.17	0.18	0.21	0.20	0.20
Mg	0.92	0.72	0.78	0.76	0.70	0.83	0.78	0.93	0.76	0.65	0.91	1.09
Mn	0.00	0.00	0.00	0.00	0.00	0.00	0.00	0.00	0.00	0.00	0.00	0.00
Ti	0.09	0.12	0.11	0.12	0.12	0.13	0.11	0.10	0.11	0.12	0.10	0.09
Al	1.82	1.85	1.82	1.84	1.78	1.84	1.82	1.81	1.84	1.82	1.80	1.72
Si	2.63	2.61	2.61	2.63	2.62	2.57	2.61	2.65	2.62	2.60	2.63	2.65
K	0.83	0.89	0.87	0.85	0.90	0.88	0.88	0.86	0.89	0.87	0.88	0.87
Na	0.06	0.05	0.05	0.05	0.03	0.03	0.04	0.04	0.02	0.06	0.05	0.03
Ca	0.00	0.00	0.00	0.00	0.00	0.00	0.00	0.00	0.00	0.00	0.00	0.00

Sample	80-178a	81-225	80-18a	80-192-2	81-234	C81-148*	C81-105	81-213	81-13a	C81-310	80-178	81-145
Weight percent*												
FeO	21.06	14.27	20.03	20.04	15.53	22.09	21.99	16.20	16.06	16.32	16.45	10.98
MgO	8.81	15.58	9.09	9.06	12.96	8.15	8.25	12.91	13.42	12.51	11.37	18.35
MnO	0.01	0.01	0.01	0.04	0.05	0.05	0.14	0.13	0.14	0.17	0.15	0.22
TiO_2	1.71	1.30	1.58	1.64	1.39	1.63	2.41	1.69	1.72	1.73	1.58	1.29
Al_2O_3	20.04	18.44	19.98	20.21	18.59	20.04	19.18	19.34	18.23	19.57	19.15	17.73
SiO_2	34.95	37.52	34.95	35.68	36.92	34.56	35.01	35.87	36.64	35.77	35.87	37.80
K_2O	8.80	8.36	8.89	8.87	9.03	9.26	9.23	9.21	9.28	9.15	9.57	8.51
Na_2O	0.34	0.45	0.35	0.30	0.44	0.25	0.18	0.30	0.24	0.34	0.25	0.37
CaO	0.01	0.01	0.01	0.00	0.01	0.00	0.01	0.00	0.01	0.01	0.00	0.03
Total	95.73	95.94	94.89	95.84	94.92	96.03	96.40	95.65	95.74	95.57	94.39	95.28
% Fe^{3+}	0.15	0.16	0.14	0.15	0.16	0.17	0.15	0.21	0.20	0.20	0.19	0.23
Cations**												
Fe^{2+}	1.13	0.73	1.09	1.07	0.81	1.16	1.18	0.79	0.79	0.81	0.84	0.51
Fe^{3+}	0.20	0.14	0.18	0.19	0.15	0.24	0.21	0.21	0.20	0.20	0.20	0.15
Mg	0.99	1.69	1.03	1.01	1.43	0.92	0.93	1.42	1.48	1.38	1.27	1.97
Mn	0.00	0.00	0.00	0.00	0.00	0.00	0.01	0.01	0.01	0.01	0.01	0.01
Ti	0.10	0.07	0.09	0.09	0.08	0.09	0.14	0.09	0.10	0.10	0.09	0.07
Al	1.78	1.58	1.79	1.78	1.62	1.79	1.71	1.68	1.59	1.71	1.70	1.51
Si	2.64	2.72	2.65	2.67	2.74	2.62	2.64	2.65	2.70	2.65	2.69	2.73
K	0.85	0.77	0.86	0.85	0.85	0.89	0.89	0.87	0.87	0.86	0.92	0.78
Na	0.05	0.06	0.05	0.04	0.06	0.04	0.03	0.04	0.03	0.05	0.04	0.05
Ca	0.00	0.00	0.00	0.00	0.00	0.00	0.00	0.00	0.00	0.00	0.00	0.00

Sample	81-70a*	80-218*	82-62	C81-244	82-12	84-147d	84-147e*	81-221*	81-175a	81-139	81-139a
Weight percent*											
FeO	15.08	13.59	9.94	9.73	9.26	7.27	6.78	8.48	2.22	1.52	1.43
MgO	12.74	14.42	16.02	17.78	17.80	18.54	20.61	17.06	22.96	22.62	22.81
MnO	0.17	0.23	0.29	0.28	0.32	0.51	0.52	1.21	0.81	0.76	0.77
TiO_2	1.54	1.09	0.60	0.61	0.72	1.01	0.96	1.95	0.88	0.60	0.56
Al_2O_3	19.39	19.72	17.70	19.13	19.89	17.64	17.27	17.48	18.87	18.32	18.46
SiO_2	35.93	36.73	36.60	37.70	37.93	38.86	38.97	37.83	37.95	39.20	39.26
K_2O	9.27	9.03	9.16	8.92	8.86	8.88	9.25	10.22	8.21	9.31	9.48
Na_2O	0.34	0.33	0.31	0.33	0.34	0.22	0.19	0.05	0.22	0.30	0.32
CaO	0.00	0.01	0.05	0.03	0.05	0.00	0.01	0.01	0.00	0.00	0.00
Total	94.46	95.15	90.67	94.51	95.17	92.93	94.56	94.29	92.12	92.63	93.09
% Fe^{3+}	0.20	0.19	0.25	0.24	0.26	0.25	0.25	0.29	0.33	0.35	0.35
Cations**											
Fe^{2+}	0.75	0.67	0.47	0.45	0.41	0.33	0.31	0.37	0.09	0.06	0.06
Fe^{3+}	0.19	0.16	0.16	0.14	0.14	0.11	0.10	0.15	0.04	0.03	0.03
Mg	1.41	1.57	1.81	1.92	1.90	2.01	2.20	1.86	2.46	2.41	2.42
Mn	0.01	0.01	0.02	0.02	0.02	0.03	0.03	0.08	0.05	0.05	0.05
Ti	0.09	0.06	0.03	0.03	0.04	0.06	0.05	0.11	0.05	0.03	0.03
Al	1.70	1.70	1.58	1.63	1.68	1.51	1.46	1.50	1.60	1.55	1.55
Si	2.68	2.69	2.78	2.73	2.72	2.83	2.79	2.76	2.73	2.80	2.80
K	0.88	0.84	0.89	0.82	0.81	0.82	0.85	0.95	0.75	0.85	0.86
Na	0.05	0.05	0.05	0.05	0.05	0.03	0.03	0.01	0.03	0.04	0.04
Ca	0.00	0.00	0.00	0.00	0.00	0.00	0.00	0.00	0.00	0.00	0.00

* % Fe^{3+} = $Fe^{3+}/(Fe^{3+} + Fe^{2+})$, estimated based on composition of coexisting oxides and Figure 3. Ratios for starred samples (*) were determined directly by Mössbauer spectroscopy and wet-chemical analysis (see text).

** Based on 11 O atoms.

TABLE 6. Microprobe analyses of biotite, Cerro Colorado, New Mexico

Sample	W83-302	W84-35	W84-86	W84-94	W84-117	W84-130	W83-300	W84-145
Weight percent*								
FeO	19.21	22.72	13.75	21.00	20.09	18.68	17.87	18.16
MgO	10.43	8.53	14.34	8.86	9.26	10.52	10.37	10.72
MnO	0.02	0.10	0.09	0.07	0.12	0.17	0.17	0.13
TiO_2	1.56	1.61	1.20	1.55	1.89	1.70	1.87	1.34
Al_2O_3	18.99	19.54	18.36	18.84	19.23	19.28	19.40	19.02
SiO_2	35.25	34.75	36.44	34.76	35.16	35.71	35.10	35.57
K_2O	9.25	9.38	8.86	9.36	9.17	9.40	9.29	9.37
Na_2O	0.23	0.31	0.28	0.24	0.16	0.29	0.28	0.31
CaO	0.04	0.01	0.01	0.04	0.01	0.02	0.03	0.01
Total	94.98	96.95	93.33	94.72	95.09	95.77	94.38	94.63
% Fe^{3+}	0.16	0.15	0.19	0.15	0.16	0.16	0.17	0.16
Cations**								
Fe^{2+}	1.021	1.217	0.697	1.144	1.069	0.982	0.939	0.964
Fe^{3+}	0.194	0.214	0.163	0.202	0.203	0.187	0.192	0.184
Mg	1.175	0.958	1.598	1.012	1.045	1.173	1.170	1.208
Mn	0.001	0.006	0.006	0.005	0.008	0.011	0.011	0.008
Ti	0.089	0.091	0.067	0.089	0.108	0.096	0.106	0.076
Al	1.692	1.735	1.618	1.702	1.717	1.700	1.730	1.694
Si	2.665	2.619	2.725	2.664	2.663	2.671	2.656	2.688
K	0.892	0.902	0.845	0.915	0.886	0.897	0.897	0.903
Na	0.034	0.045	0.041	0.036	0.023	0.042	0.041	0.045
Ca	0.003	0.001	0.001	0.003	0.001	0.002	0.002	0.001

* % $Fe^{3+} = Fe^{3+}/(Fe^{3+} + Fe^{2+})$, estimated based on composition of coexisting oxides and Figure 3.
** Based on 11 O atoms.

librium between garnet and biotite, given the relationship shown in Figure 3.

X_{sps} vs. X_{Ti}^{Bt}. A strong negative covariance exists between X_{sps} and X_{Ti}^{Bt} (correlation coefficient > -0.6). This is not surprising considering the correlations discussed above and well-documented positive correlation between Ti and Fe/(Mg + Fe) in biotite (Guidotti, 1984). This relationship suggests that it may be difficult to separate the effects of Mn mixing in garnet and those of Ti mixing in biotite.

X_{sps} vs. f_{O_2}. Chinner (1960) and Guidotti (1984) noted

TABLE 7. Selected ilmenite-hematite analyses and assemblages*

Pecos Baldy, New Mexico	77-85B	76-420	77-81E	77-41	78-22A	77-73	77-23	83-45	77-45	77-46D	76-437	77-45	84-1622	84-162
$X(Fe_2O_3)$	0.00	0.02	0.04	0.03	0.02	0.00	0.06	0.00	0.67	0.18	0.00	0.20	0.72	0.67
$X(FeTiO_3)$	1.00	0.97	0.93	0.97	0.96	0.98	0.86	0.98	0.32	0.79	0.88	0.77	0.27	0.33
$X(MnTiO_3)$	0.00	0.01	0.07	0.00	0.02	0.02	0.13	0.02	0.01	0.03	0.12	0.02	0.01	0.01
Rutile	—	X	X	X	X	—	X	—	—	—	—	X	—	—
Magnetite	—	—	—	—	—	—	—	—	—	X	—	—	—	—
Rio Mora, New Mexico	**80-46**	**80-46b**	**80-30**	**80-187**	**80-20**	**81-225**	**81-225**	**80-1922**	**81-234s**	**C81-148**	**C81-105**	**81-213**	**C81-310**	**80-218**
$X(Fe_2O_3)$	0.016	0.009	0.000	0.000	0.028	0.109	0.732	0.000	0.123	0.073	0.067	0.636	0.422	0.716
$X(FeTiO_3)$	0.983	0.986	0.960	0.933	0.967	0.883	0.268	0.969	0.859	0.915	0.863	0.352	0.567	0.280
$X(MnTiO_3)$	0.001	0.005	0.040	0.017	0.005	0.008	0.000	0.031	0.018	0.012	0.071	0.012	0.011	0.004
Rutile	—	—	X	X	X	—	—	X	—	—	—	—	—	—
Magnetite	—	—	—	—	—	X	X	—	X	X	X	X	X	—
Rio Mora, New Mexico (continued)	**82-62**	**C81-244**	**82-12**	**84-147e**	**84-147d**	**81-221**	**81-175a**	**81-139**	**81-139a**					
$X(Fe_2O_3)$	0.850	0.832	0.844	0.802	0.796	0.872	0.959	0.978	0.979					
$X(FeTiO_3)$	0.146	0.165	0.146	0.191	0.198	0.122	0.035	0.003	0.009					
$X(MnTiO_3)$	0.003	0.003	0.010	0.007	0.006	0.006	0.006	0.019	0.012					
Rutile	—	—	—	X	—	X	—	X	—					
Magnetite	X	—	—	—	—	—	—	—	—					
Cerro Colorado, New Mexico	**W83-302**	**W84-86**	**W84-86**	**W84-94b**	**W84-129**	**W84-130**	**W84-130**	**W84-145**	**W84-145**	**W84-75**				
$X(Fe_2O_3)$	0.06	0.65	0.11	0.09	0.11	0.14	0.77	0.10	0.75	0.68				
$X(FeTiO_3)$	0.93	0.34	0.87	0.89	0.87	0.84	0.23	0.89	0.25	0.31				
$X(MnTiO_3)$	0.01	0.01	0.02	0.02	0.01	0.01	0.01	0.01	0.00	0.01				
Rutile	—	—	—	—	—	—	—	—	—	—				
Magnetite	X	X	X	X	X	X	X	X	X	X				

Note: X indicates the presence of rutile or magnetite in the assemblage.
* Mole fractions calculated according to the method of Rumble (1973).

TABLE 6.—*Continued*

W85-195	W84-58	W84-153	W84-87	W85-253	W84-75	W83-242	W84-133	W85-254
17.52	17.20	14.70	16.63	14.38	13.75	15.73	13.75	10.22
11.37	11.27	12.96	11.61	12.86	13.71	12.09	14.01	16.44
0.14	0.18	0.19	0.19	0.17	0.15	0.22	0.17	0.31
1.42	1.44	1.37	1.79	1.42	1.27	1.31	1.34	1.02
19.59	19.70	19.30	19.30	19.49	19.08	19.75	19.23	18.99
35.15	35.66	36.06	35.76	36.64	36.27	35.76	36.28	37.00
9.22	9.31	8.94	9.56	9.35	9.20	9.36	9.45	9.11
0.24	0.26	0.33	0.23	0.30	0.31	0.26	0.34	0.36
0.01	0.00	0.03	0.00	0.01	0.01	0.01	0.01	0.02
94.66	95.02	93.88	95.07	94.62	93.75	94.49	94.58	93.47
0.17	0.17	0.20	0.17	0.20	0.20	0.20	0.20	0.23
0.915	0.893	0.734	0.862	0.712	0.686	0.786	0.681	0.484
0.187	0.183	0.183	0.177	0.178	0.171	0.196	0.170	0.144
1.276	1.256	1.442	1.293	1.418	1.523	1.346	1.546	1.802
0.009	0.011	0.012	0.012	0.011	0.009	0.014	0.011	0.019
0.080	0.081	0.077	0.101	0.079	0.071	0.074	0.075	0.056
1.738	1.737	1.698	1.700	1.700	1.676	1.738	1.678	1.646
2.645	2.667	2.692	2.672	2.711	2.704	2.670	2.685	2.721
0.885	0.888	0.851	0.911	0.883	0.875	0.892	0.892	0.855
0.035	0.038	0.048	0.033	0.043	0.045	0.038	0.049	0.051
0.001	0.000	0.002	0.000	0.001	0.001	0.001	0.001	0.002

that the manganese content of garnet increases with O_2. The samples from New Mexico show the same behavior, as illustrated by the correlation between Mn in garnet and $X_{Fe_2O_3}$ in ilmenite-hematite solid solution (Fig. 6). This correlation is also a result of partitioning relationships. An increase in f_{O_2} is associated with a decrease in $Fe^{2+}/(Fe^{2+} + Mg)$ of the coexisting silicate phases, including biotite and garnet, which in turn is coupled to increases in X_{sps} (Figs. 3 and 4).

It should be stressed that the linear relationship between f_{O_2} and X_{sps} would not be expected to characterize all regions or even all samples from New Mexico. To a

TABLE 8. Correlation coefficients for compositional variables in Equation 3

Pecos Baldy, New Mexico	X_{sps}	X_{grs}	$(X_{alm} - X_{prp})$	X_{Ti}^{Bt}	$X_{Fe^{3+}}^{Bt*}$	X_{Al}^{Bt*}	$(X_{Fe} - X_{Mg})^{Bt}$
X_{sps}	1.0						
X_{grs}	0.592	1.0					
$(X_{alm} - X_{prp})$	−0.964	−0.729	1.0				
X_{Ti}^{Bt}	−0.618	−0.665	0.737	1.0			
$X_{Fe^{3+}}^{Bt*}$	0.250	0.058	−0.191	−0.079	1.0		
X_{Al}^{Bt*}	−0.852	−0.636	0.889	0.663	−0.270	1.0	
$(X_{Fe} - X_{Mg})^{Bt}$	−0.876	−0.776	0.970	0.819	−0.113	0.861	1.0
$\ln K_D^{Grt-Bt}$	−0.828	−0.744	0.841	0.719	−0.258	0.727	0.823
Rio Mora, New Mexico	X_{sps}	X_{grs}	$(X_{alm} - X_{prp})$	X_{Ti}^{Bt}	$X_{Fe^{3+}}^{Bt*}$	X_{Al}^{Bt*}	$(X_{Fe} - X_{Mg})^{Bt}$
X_{sps}	1.0						
X_{grs}	0.423	1.0					
$(X_{alm} - X_{prp})$	−0.952	−0.541	1.0				
X_{Ti}^{Bt}	−0.780	−0.280	0.844	1.0			
$X_{Fe^{3+}}^{Bt*}$	−0.640	−0.271	0.728	0.744	1.0		
X_{Al}^{Bt*}	−0.601	−0.784	0.741	0.439	0.431	1.0	
$(X_{Fe} - X_{Mg})^{Bt}$	−0.903	−0.553	0.986	0.874	0.745	0.752	1.0
$\ln K_D^{Grt-Bt}$	−0.680	−0.741	0.706	0.580	0.355	0.646	0.734
Cerro Colorado, New Mexico	X_{sps}	X_{grs}	$(X_{alm} - X_{prp})$	X_{Ti}^{Bt}	$X_{Fe^{3+}}^{Bt*}$	X_{Al}^{Bt*}	$(X_{Fe} - X_{Mg})^{Bt}$
X_{sps}	1.0						
X_{grs}	−0.449	1.0					
$(X_{alm} - X_{prp})$	−0.827	0.166	1.0				
X_{Ti}^{Bt}	−0.682	0.339	0.838	1.0			
$X_{Fe^{3+}}^{Bt*}$	−0.542	0.562	0.580	0.720	1.0		
X_{Al}^{Bt*}	0.359	0.071	−0.255	0.195	0.139	1.0	
$(X_{Fe} - X_{Mg})^{Bt}$	−0.754	0.337	0.924	0.932	0.773	−0.001	1.0
$\ln K_D^{Grt-Bt}$	−0.480	0.573	0.084	0.313	0.515	0.201	0.300

* Octahedral cations only.

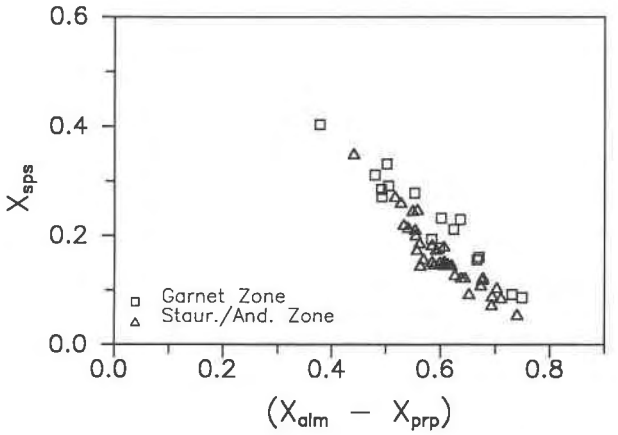

Fig. 5. X_{sps} vs. $(X_{alm} - X_{prp})$ for garnets from the Waterville Formation, Maine (Ferry, 1980) (slope = −0.89, x-intercept = 0.77, $r^2 = 0.83$). Note the similar linear trend but different slope from data from New Mexico (Fig. 3).

large extent, the correlation may reflect the generally oxidized nature of the Mn-rich sedimentary protoliths. However, where present, this relationship can seriously obscure the mixing behavior of other components. In most samples from New Mexico, as X_{sps} increases, an increasing percentage of Fe in biotite is Fe^{3+} (Fig. 7). If this Fe^{3+} is not subtracted from total Fe, as in typical microprobe analyses, $K_D^{Bt\text{-}Grt}$ and estimated temperature will be erroneously high. The effect is opposite of that predicted for nonideal mixing of Mn in magnesium-iron garnet and thus partially cancels the effect of Mn on K_D, creating the erroneous impression that Mn mixing is more nearly ideal (Williams and Grambling, 1984).

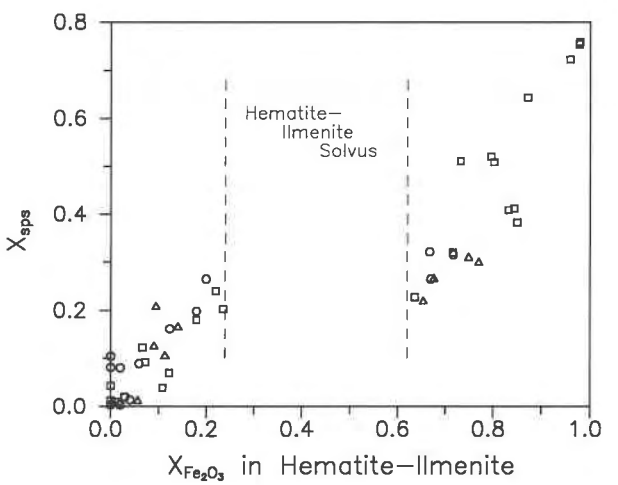

Fig. 6. Mole-fraction spessartine in garnet vs. mole-fraction hematite in hematite-ilmenite. Constructed from recalculated microprobe analyses in Tables 1–3 and 7. Note that the plot is not a rigorous representation of an isothermal solvus because the three study areas crystallized at different peak metamorphic temperatures.

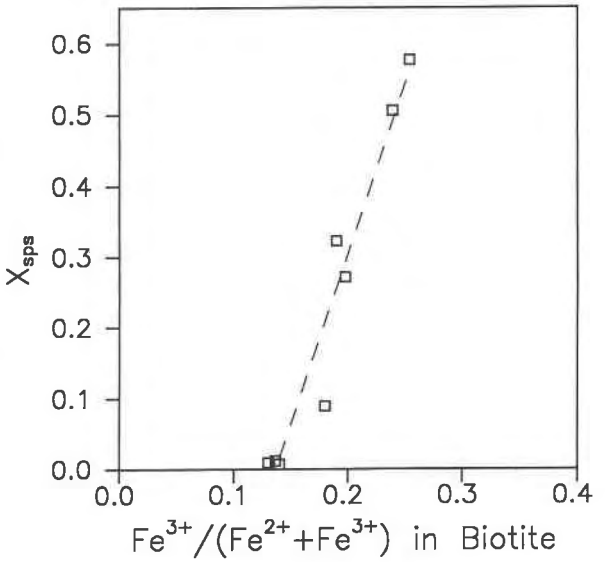

Fig. 7. Mole-fraction spessartine in garnet vs. $Fe^{3+}/(Fe^{3+} + Fe^{2+})$ in biotite. Fe^{3+}/Fe^{2+} ratios are from wet-chemical and Mössbauer analyses of biotite separates. Garnets were analyzed with the electron microprobe (Table 2). All samples are from the Rio Mora area.

Finally, for the regression analyses that follow, it is important to note that, although $Fe^{3+}/(Fe^{3+} + Fe^{2+})$ in biotite is positively correlated with X_{sps} in the New Mexico rocks, $X_{Fe^{3+}}^{Bt}$ does not show the same relationship. As noted above, the number of Fe^{3+} cations is nearly constant, decreasing slightly with increasing X_{sps}.

***X_{sps}* vs. garnet-biotite K_D.** Table 8 and Figure 8 document a negative correlation between X_{sps} and $K_D^{Grt\text{-}Bt}$. This correlation suggests that Mn mixes nonideally in garnet. However, it is difficult to use the data in Table 8 directly to calculate the magnitude of the Mn-Mg interaction parameter because most other compositional variables are correlated to some degree with X_{sps}. Therefore, the negative slopes in Figure 8 incorporate the combined nonideal mixing effects of a number of components in garnet and biotite.

Six specimens from Rio Mora have X_{sps} between 0.50 and 0.76. These samples, not shown in Figure 8, display a dramatic reversal of the X_{sps} vs. $K_D^{Grt\text{-}Bt}$ trend; as X_{sps} rises from 0.50 to 0.76, K_D rises. These samples are shown on Figure 9, but because several of the garnets contain slightly higher X_{grs}, ln K_D has been corrected for the effects of nonideal Ca mixing (W_{Ca}^{Grt} = 12550 J/mol). The reason for this reversal is unclear to us. Although a number of these samples have relatively high X_{grs}, no direct relationship exists between X_{grs} and ln K_D. As expected, these samples have garnets and biotites characterized by high Mg/(Mg + Fe) and are associated with ilmenite-hematite oxides rich in the hematite component. However, the ln K_D reversal cannot be explained by asymmetric mixing behavior of magnesium garnet according to any recently proposed model. Further, although it is difficult to esti-

mate the amount of Fe^{3+} in these low-Fe biotites, and K_D is extremely sensitive to errors in the estimate, Fe^{3+} was determined directly in two of these biotite samples, and so errors in the Fe^{3+}/Fe^{2+} ratios do not seem to be responsible for the reversals. Also, because of the low total Fe, $X^{Bt}_{Fe^{3+}}$ is extremely small in these biotites, so nonideal Fe^{3+} mixing would also not seem to be responsible for the reversal. At present, we suspect that the reversals may relate to an important change in the mixing behavior of garnet or biotite at high X_{sps} and high f_{O_2}. Because of the dramatic nature of the reversal and because most of these samples have slightly elevated X_{grs}, we have elected to exclude them from our regression analyses and to restrict our conclusions to garnets with X_{sps} less than 0.50.

Regression techniques for multicolinear data sets

Statistical regression of multicolinear data can lead to large standard deviations for the estimated coefficients because variation produced by one coefficient is, to varying degrees, attributed to another coefficient. In the case of garnet, some variation in ln K_D due to nonideal Mn mixing might be attributed erroneously to another coefficient, such as $(X_{alm} - X_{prp})$. Further, nonideality may be unrecognized because the effects of one coefficient may cancel the effects of another. For example, the predicted effects of nonideal mixing of Ti in biotite and Mn in garnet are opposite in sign (Dallmeyer, 1974; Indares and Martignole, 1985). Because of the correlation between X_{sps} and X^{Bt}_{Ti}, these effects will tend to cancel and obscure the true mixing behavior of both components.

Traditional least-squares multiple regression analysis may not reveal the presence or effects of multicolinearity. Hence, two alternate approaches have been used here. The first involves elimination of the least important coefficients from the model, fixing the value of coefficients that are reasonably well known, or both. The second involves the use of a regression technique that yields biased rather than unbiased estimates of the model coefficients (ridge regression, Devore, 1982). A biased regression may reduce the standard deviation of regression coefficients and highlight those coefficients not important for the regression model.

For this study, multiple regressions (least-squares and biased regressions) were carried out in a backward stepwise manner: regression coefficients were subtracted from the model one at a time in order to evaluate the influence of any one on the regression model. The least significant coefficients were eliminated from the model one at a time and the remaining coefficients re-regressed. Coefficients were evaluated on the basis of their t ratio. For any coefficient i, $t_i = \beta_i/\sigma_i$ where β is the value of the estimated coefficient and σ is the standard deviation of that coeffi-

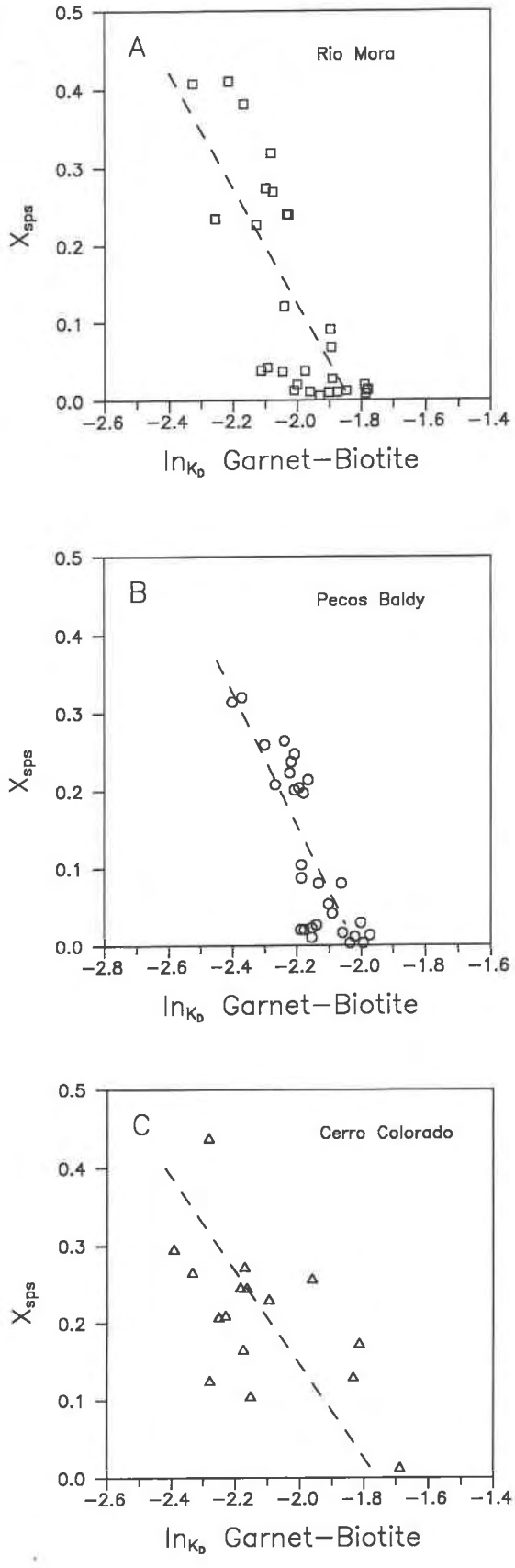

→

Fig. 8. Mole-fraction spessartine in garnet vs. ln $K_D^{Grt\text{-}Bt}$ where Fe^{Bt} includes only Fe^{2+}. Fe^{3+} contents of biotite were estimated from Figure 2. Each point represents one sample.

cient (Devore, 1982). Coefficients with t ratios less than 2 are not distinguishable from zero at the 95% confidence level and were not considered significant.

Simplification of regression model

Several terms can be eliminated from Equation 3 because they are of only minor importance in samples from New Mexico. $W_{MgFe}(X_{Fe} - X_{Mg})^{Bt}$ can be eliminated because W^{Bt}_{MgFe} is suspected to be near zero (see above). $\Delta W_{Mn}(X_{Mn})^{Bt}$ can be eliminated because X^{Bt}_{Mn} is near zero. Both of these terms are strongly correlated with X_{sps} and $(X_{alm} - X_{prp})$. Readers should note that, by eliminating these terms, any nonideal behavior actually carried by them will be assigned to other coefficients.

Because X_{grs} is small (<0.10) and ΔW^{Grt}_{Ca} has been constrained at approximately 12550 J/mol in other studies (Ganguly and Saxena, 1984; Ganguly and Kennedy, 1974), the term $\Delta W_{Ca}(X_{grs})$ has been incorporated into the left side of the equation for most of the regressions that follow. With these simplifications, Equation 3 can be rewritten:

$$-RT \ln K_D - 12550(X_{grs}) = -RT \ln K_{eq} + [W_{MgFe}(X_{alm} - X_{prp}) + \Delta W_{Mn}(X_{sps})]^{Grt} - [\Delta W_{Ti}(X_{Ti}) - \Delta W_{Al}(X_{Al}) - \Delta W_{Fe^{3+}}(X_{Fe^{3+}})]^{Bt}. \quad (5)$$

Equation 5 may be simplified further. X^{Bt}_{Ti} and $X^{Bt}_{Fe^{3+}}$ are both very small and vary only slightly. X^{Bt}_{Al}, although significant in magnitude, is also nearly constant. If these components are eliminated, Equation 5 becomes

$$-RT \ln K_D - 12550(X_{grs}) = -RT \ln K_{eq} + [W_{MgFe}(X_{alm} - X_{prp}) + \Delta W_{Mn}(X_{sps})]^{Grt}. \quad (6)$$

These final simplifications are not completely justified because none of the eliminated variables are rigorously constant. Therefore, regression analyses have been carried out on both Equations 5 and 6. Correlation matrices have been constructed for the three data sets incorporating the left side of Equations 5 and 6. However, correlation coefficients are not significantly different from those in Table 8, and thus they are not reproduced here. Readers should note that the two remaining nonideal mixing terms in Equation 6 are associated with the two most strongly correlated compositional parameters, $(X_{alm} - X_{prp})$ and X_{sps}, and thus even with all of the simplifications, regression analyses of Equation 6 must be affected by multicolinearity.

Biased multiple regression (ridge regression)

Ridge regression is based on the concept that "a biased estimator with a small variance may be preferred over an unbiased estimator with a large variance" (Devore, 1982, p. 513). The technique, described by Devore (1982, p. 513–516), is briefly summarized here. Ridge regression uses a biasing constant, c, which is multiplied by the covariance of the individual compositional variables. As c increases, the amount of bias in the estimated coefficients increases. Theoretically for multicolinear data, as c increases, the total mean-squared error of the ridge estimators decreases to a minimum and then increases. Near this optimum (minimum) value, the ridge estimators may represent an improvement on the least-squares estimators. However, the optimum value of c is unknown because it depends on the unknown regression parameters. Its value must be selected based on the sample data. Typically, a plot of c vs. the ridge-estimated coefficients (ridge trace) is constructed and c is chosen as the smallest value for which the estimators have stabilized. The ridge trace for a ridge regression of data from Pecos Baldy presents an example (Fig. 10). Typical of all New Mexico data, ridge coefficients change dramatically at first, but then quickly stabilize at a very small value of c. Thus, with a rather small amount of bias, significant improvement can apparently be made to the estimated coefficients.

As noted by Devore (1982), statisticians disagree about which value of the biasing constant (c) to select. The choice of the stabilization point on the ridge trace is somewhat arbitrary. Even if ridge coefficients are not accepted, however, ridge regression analysis can be useful for selecting coefficients in a multicovariant data set that are least important. Coefficients that quickly converge on zero with increasing c are candidates for elimination from the regression model. The remaining coefficients can be reregressed using either least-squares or additional ridge regressions.

Regression results

Results of regression analyses for each of the three study areas in New Mexico are summarized in Table 9.

Ca mixing in garnet. Preliminary stepwise regression analyses carried out using Equation 3 (Table 9, Model 1) yield values of ΔW_{Ca} of approximately 20000 (σ = 5000) J/mol for least-squares or 14000 (σ = 5000) J/mol for ridge regressions. The latter estimate is indistinguishable from the value of ΔW^{Grt}_{Ca} = 12550 (σ = 2090 J/mol), suggested by Ganguly and Saxena (1984). It provides an example of the success of the ridge regression technique. The larger value of the least-squares estimate probably reflects the positive correlation between X_{sps} and X_{grs} observed in the data (Table 8).

Ti,Al,Fe^{3+} mixing in biotite. Stepwise regressions using Equation 5 suggest that octahedral Fe^{3+} and Al in biotite do not significantly contribute to the regression model. This does not require that these components mix ideally, but only that their nonideal effects do not account for variation in ln K_D within the range of compositions examined.

The term ΔW^{Bt}_{Ti} is significant in most least-squares regressions, and it is significant in several models using ridge regression. However, the derived coefficients exceed −50000 J/mol, which seems unreasonable. Using regression analyses of natural data, Indares and Martignole (1985) suggested that ΔW^{Bt}_{Ti} is approximately −30000 J/mol. We suspect that the large values obtained here are exaggerated because of multicolinearity. This is suggested

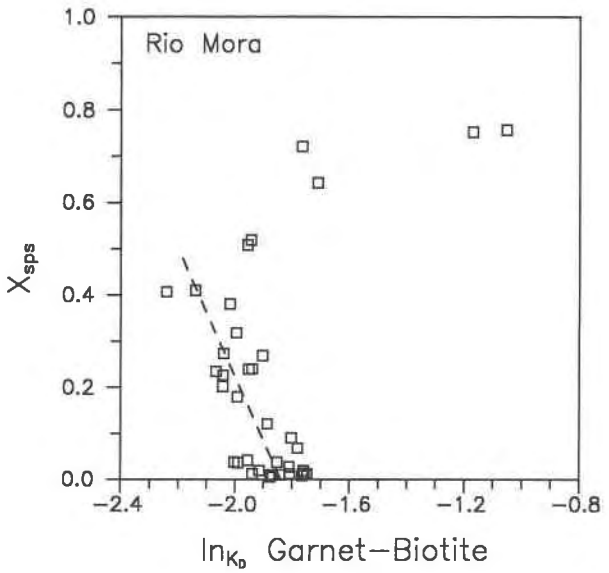

Fig. 9. Mole-fraction spessartine in garnet vs. ln $K_D^{Grt\text{-}Bt}$ for all samples from Rio Mora. The ln K_D values have been corrected for the effects of nonideal Ca mixing ($W_{Ca}^{Grt} = 12500$ J/mol). Fe^{Bt} includes only Fe^{2+}; Fe^{3+} estimates are from Figure 2. Samples with X_{sps} greater than 0.5 were excluded from all regression analyses (see text).

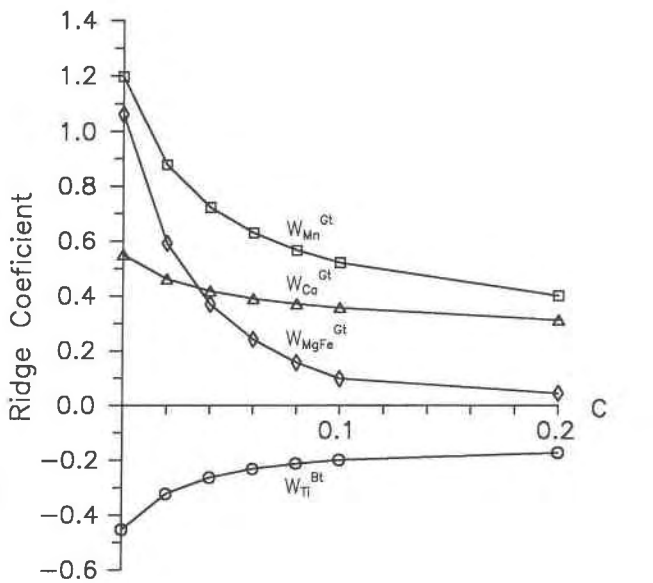

Fig. 10. Ridge trace for ridge regression of ln K_D against X_{sps}, X_{grs}, $(X_{alm} - X_{prp})$, and X_{Ti}^{Bt} from Pecos Baldy (Table 9, Model 1). Regression data (mole fractions) were normalized to the mean and standard deviation of the particular variable (Devore, 1982). Increasing c (biasing constant) produces increasingly biased estimates. The regression coefficients are chosen at the minimum value of c where relative stability occurs. Coefficients that approach zero are relatively unimportant to the regression model.

by the tendency for X_{Ti}^{Bt} to be eliminated from most ridge regression models. It is possible that slight alteration or reequilibration of biotite is reflected in a decrease in X_{Ti}^{Bt} and a slight reduction in $K_D^{Grt\text{-}Bt}$. This effect could contribute to the large values for ΔW_{Ti}^{Bt} in the regression analyses. Because of the strong possibility that other factors are contributing to the derived value of ΔW_{Ti}^{Bt}, we have chosen to eliminate it from our subsequent regressions. Although not rigorously justified, this simplification will not significantly influence our conclusions. With a modest value of ΔW_{Ti}^{Bt}, such as -30000 J/mol (Indares and Martignole, 1985), the small magnitude of X_{Ti}^{Bt} in our samples minimizes the importance of this term.

Mn and Fe-Mg mixing in garnet. Regression analyses using Equation 6 were carried out by excluding W_{Ti}, $W_{Fe^{3+}}$, and W_{Al} in biotite from Model 2 in Table 9. Assuming that Fe-Mg mixing in garnet follows symmetric simple mixture behavior (i.e., W_{MgFe}^{Grt} is constant), these analyses consistently yield small values for ΔW_{Mn}^{Grt} (5000 J/mol) and near zero values for W_{MgFe}^{Grt}. This indicates that the minimum sums of both the squared residuals (SSE) and mean-squared error (MSE) occur when most variation due to nonideal mixing is incorporated into the ΔW_{Mn}^{Grt} term. Because of the near perfect correlation between X_{sps} and $(X_{alm} - X_{prp})$, a range of paired values of ΔW_{Mn}^{Grt} and W_{MgFe}^{Grt} results in only slightly larger model errors. Error (SSE and MSE) and the regression variance both increase monotonically, but rather slowly, with increasing ΔW_{Mn}^{Grt}. The data allow but do not require ideal Mg-Fe mixing in garnet.

Several attempts were made to incorporate into the regression analyses the hypothesis that Mg-Fe mixing behavior in garnet is asymmetric (Ganguly and Saxena, 1984; Hackler and Wood, 1989). The first attempt utilized regressions of Equation 6 with W_{MgFe}^{Grt} fixed according to Equation 4 and the Fe-Mg mixing parameters of either Ganguly and Saxena (Table 9, Model 3a) or Hackler and Wood (Table 9, Model 3b). The parameters of Ganguly and Saxena (1984) imply a significant amount of Mg-Fe nonideality, approximately 8000 J/mol for Fe-rich garnets. With this model, ΔW_{Mn}^{Grt} is 19780, 19630, and 17570 J/mol for Pecos Baldy, Rio Mora, and Cerro Colorado, respectively (Table 9, Model 3a), values considerably larger than those suggested by Ganguly and Saxena (1984). The parameters of Hackler and Wood imply only a moderate amount of Mg-Fe nonideality, less than 2000 J/mol for Fe-rich garnets. With this model, ΔW_{Mn}^{Grt} is 7120, 7630, and 9720 J/mol for Pecos Baldy, Rio Mora, and Cerro Colorado, respectively (Table 9, Model 3b). The coefficient of multiple determination (r^2) for these models are impressive, approximately 0.90 for Model 3a and 0.80 for Model 3b, and considerably higher than the values of 0.60 to 0.70 derived from Models 1 and 2 in Table 9. However, the SSE and MSE of the regressions are largest for Model 3a, intermediate for Model 3b, and smallest for models assuming ideal Mg-Fe mixing.

It is suspected that neither r^2 nor regression error (SSE or MSE) can be used to evaluate the success of the various

TABLE 9. Summary of least squares and ridge regression analyses

Model 1: Regression using Equation 3

Data source	Reg. type	Garnet			Biotite			SSE	MSE	R^2	s	F	C
		ΔW_{Mn}	ΔW_{Ca}	W_{MgFe}	ΔW_{Ti}	$\Delta W_{Fe^{3+}}$	ΔW_{Al}						
PB	L-Sq	10458	20605	6080	−77 714	*	*	1 993 781	83 074	0.85	288	33	
	σ	(2704)	(5448)	(2239)	(27 414)								
PB	Ridge	5425	14080	*	*	*	*	2 288 887	95 370	0.82	309	28	0.03
	σ	(1921)	(5058)										
PB	L-Sq	3745	14176	*	*	*	*	2 816 409	108 323	0.78	329	46	
	σ	(711)	(4185)										
RM	L-Sq	8498	22340	1926	−47 571	*	*	5 886 473	245 270	0.78	495	21.5	
	σ	(2151)	(5264)	(1926)	(20 042)								
RM	Ridge	4347	14561	*	*	*	*	7 702 576	296 253	0.72	544	33	0.03
	σ	(805)	(4566)										
CC	L-Sq	17921	*	11615	*	*	*	13 536 325	966 880	0.54	983	8.2	
	σ	(4444)		(3772)									
CC	Ridge	11935	*	6744	*	*	*	15 385 584	1 098 970	0.49	1048	6.4	0.12
	σ	(3877)		(3291)									

Model 2: Regression using Equation 5

Data source	Reg. type	Garnet			Biotite			SSE	MSE	R^2	s	F	C
		ΔW_{Mn}	ΔW_{Ca}	W_{MgFe}	ΔW_{Ti}	$\Delta W_{Fe^{3+}}$	ΔW_{Al}						
PB	L-Sq	8197		3928	−75 019	*	*	2 170 062	86 802	0.73	295	22	
	σ	(2276)		(1747)	(27 971)								
PB	L-Sq	5011		*	N.I.	*	*	2 794 454	107 479	0.65	328	24	
	σ	(2160)											
PB	L-Sq	3930		N.I.	N.I.	*	*	2 823 423	104 571	0.65	3236	49	
	σ	(563)											
PB	Ridge	4073		*	*	*	*	2 461 191	98 448	0.69	314	19	0.04
	σ	(1516)											
RM	L-Sq	4581		*	*	*	*	7 752 977	287 147	0.60	536	39	0.02
	σ	(729)											
CC	L-Sq	20423		13008	*	*	*	15 913 332	1 136 666	0.57	1066	9	
	σ	(4818)		(4089)									
CC	L-Sq	7724		N.I.	*	*	*	27 414 109	1 827 607	0.25	1351	5	
	σ	(3419)											
CC	Ridge	12966		6970	*	*	*	18 772 777	1 340 912	0.50	1158	7	0.14
	σ	(4173)		(3542)									

Model 3a: Regression using Equation 6, W^{Grt}_{FeMg} fixed according to Equation 4, Fe-Mg mixing model of Ganguly and Saxena (1984)

Data source	Reg. type	Garnet			Biotite			SSE	MSE	R^2	s	F	C
		ΔW_{Mn}	ΔW_{Ca}	W_{MgFe}	ΔW_{Ti}	$\Delta W_{Fe^{3+}}$	ΔW_{Al}						
PB	L-Sq	16518			−165 827	*	*	4 341 024	166 962	0.97	409	403	
	σ	(905)			(28 432)								
PB	L-Sq	19779			N.I.	*	*	10 020 521	371 130	0.93	609	348	
	σ	(1061)											
PB	Ridge	No improvement on least-squares model											
RM	L-Sq	14420			−99 698	*	*	14 898 403	573 015	0.94	757	191	
	σ	(1585)			(23 025)								
RM	L-Sq	19634			N.I.	*	*	25 640 970	949 665	0.89	974	219	
	σ	(1326)											
RM	Ridge	No improvement on least-squares model											
CC	L-Sq	18655			560 737	*	*	14 991 416	1 070 815	0.77	1034	23	
	σ	(2815)			(53 303)								
CC	L-Sq	17566			N.I.	*	*	16 176 427	1 078 428	0.74	1038	44	
	σ	(2627)											
CC	Ridge	No improvement on least-squares model											

regression analyses with respect to Mg-Fe mixing in garnet. Variations in SSE, MSE, and r^2 result, in part, from a model-dependent magnifying effect: constant errors in microprobe analyses produce increasing SSE, MSE, and r^2 as W^{Grt}_{MgFe} and ΔW^{Grt}_{Mn} increase. SSE and MSE increase because microprobe data are multiplied by W^{Grt}_{MgFe} in the regression model. Thus, when W^{Grt}_{MgFe} is fixed at a large value, scatter in the data leads to increased scatter in the regression solution. The multiple correlation coefficient (r^2) is defined as 1 − (SSE/SST) (Devore, 1982) where SST is the sum of the squared total error of the dependent variable. As the paired values of W^{Grt}_{MgFe} and ΔW^{Grt}_{Mn} increase, both SSE and SST increase because of the magnifying effect described above. However, SST increases

TABLE 9.—*Continued*

Model 3b: Regression using Equation 6, W^{Grt}_{FeMg} fixed according to Equation 4, Fe-Mg mixing model of Hackler and Wood (1989)

Data source	Reg. type	Garnet			Biotite			SSE	MSE	R^2	s	F	C
		ΔW_{Mn}	ΔW_{Ca}	W_{MgFe}	ΔW_{Ti}	$\Delta W_{Fe^{3+}}$	ΔW_{Al}						
PB	L-Sq	5907			−58 749	*	*	2 212 171	85 083	0.89	292	102	
	σ	(646)			(20 297)								
PB	L-Sq	7122			N.I.	*	*	2 925 041	108 334	0.85	329	154	
	σ	(573)											
PB	Ridge	No improvement on least-squares model											
RM	L-Sq	5983			−31 471	*	*	6 757 682	259 910	0.83	509	63	
	σ	(1067)			(15 507)								
RM	L-Sq	7629			N.I.	*	*	7 828 160	2 899 315	0.80	538	108	
	σ	(732)											
RM	Ridge	No improvement on least-squares model											
CC	L-Sq	12067			120 587	*	*	18 103 033	1 293 073	0.53	1137	8	
	σ	(3093)			(58 574)								
CC	L-Sq	9724			N.I.	*	*	23 583 475	1 572 231	0.39	1254	10	
	σ	(3171)											
CC	Ridge	No improvement on least-squares model											

Model 4: Regression using Equation 7

Data source	Reg. type	Garnet				SSE	MSE	R^2	s	F
		ΔW_{Mn}	ΔW_{Ca}	W_{MgFe}	W_{FeMg}					
PB	L-Sq	4853		N.I.	632	2 767 536	608 010	0.65	326	24
	σ	(2150)			(1418)					
RM	L-Sq	6117		N.I.	1067	7 513 286	288 969	0.60	540	20
	σ	(2071)			(1339)					
CC	L-Sq	21472		N.I.	12556	17 667 785	1 261 980	0.57	1121	9.2
	σ	(1210)			(1028)					

Note: L-Sq: stepwise least-squares regression; Ridge: stepwise ridge regression; PB: Pecos Baldy study area; RM: Rio Mora study area; CC: Cerro Colorado study area; N.I.: variable not included in regression analysis; *: variable eliminated during stepwise regression (see text); SSE: sum of squared error; MSE: mean-squared error; R^2: coefficient of multiple determination; s: regression standard deviation; F: F statistic (Devore, 1982); and C: ridge constant (biasing constant for ridge regressions).

more rapidly than SSE, which causes r^2 to increase. Thus, the increase in r^2 and regression error may simply be an artifact of greater sensitivity of the dependent variable to routine analytical errors, instead of a better regression model. Consequently, one cannot determine uniquely which statistical model is more appropriate.

As a second attempt to evaluate the asymmetric mixing hypothesis, Equation 6 can be rewritten to explicitly incorporate the symmetric approximation (Equation 4) to asymmetric Mg-Fe mixing in garnet, maintaining $W_{Mg\text{-}Fe}$ and $W_{Fe\text{-}Mg}$ as variables:

$$\begin{aligned} -RT \ln K_D - 12550(X_{grs}) \\ = -RT \ln K_{eq} + [f(X_{prp})W_{Fe\text{-}Mg} \\ + f(X_{alm})W_{Mg\text{-}Fe} + \Delta W_{Mn}(X_{sps})]^{Grt} \end{aligned} \quad (7)$$

with $f(X_i) = [X_i/(X_{prp} + X_{alm})](X_{alm} - X_{prp})$. Preliminary least-squares stepwise regressions of $\ln K_D$ against the three compositional variables in Equation 7 yielded large negative values for $W_{Mg\text{-}Fe}$ and $W_{Fe\text{-}Mg}$. These values, which contradict the estimates of Ganguly and Saxena (1984), Geiger et al. (1987), and Hackler and Wood (1989), seem unreasonable. This is not surprising, considering the highly correlated nature of the X_{alm}- and X_{prp}-dependent variables.

Ridge regression suggests a third way to treat the data. As the ridge regression biasing constant (c) increases, the $f(X_{prp})(W_{Fe\text{-}Mg})$ term quickly converges on zero, suggesting that it may not be important to the regression model. This is consistent with all existing mixing models; all propose that $W^{Grt}_{Fe\text{-}Mg}$ is less than 1000 J/mol. Elimination of $W^{Grt}_{Fe\text{-}Mg}$ from the model yields small values for the two remaining interaction parameters, $W^{Grt}_{Mg\text{-}Fe}$ and ΔW^{Grt}_{Mn} (Table 9, Model 4). The results are similar to those obtained using Equations 5 or 6 with no significant improvement in the regression statistics.

Toward independent estimates of ΔW^{Grt}_{Mn} and W^{Grt}_{MgFe}

Least-squares and ridge regression analyses suggest that Equation 6 characterizes nonideal mixing in garnet and biotite from New Mexico. Nonideality in the mixing of Ti, Al, and Fe^{3+} into Fe^{2+}-Mg biotite has little or no effect within the compositional range of biotite samples treated here, but the Ca, Mn, and Fe-Mg interaction parameters for garnet are all nonzero. The magnitude of Ca nonideality (ΔW^{Grt}_{Ca}) seems to fall near 12550 J/mol, as suggested by Ganguly and Saxena (1984).

As noted above, garnet mixing behavior within each individual study area can be described with a range of paired ΔW^{Grt}_{Mn} and W^{Grt}_{MgFe} values. The relationship between

TABLE 10. Suggested interaction parameters (J/mol, one-site basis)

	Model 1		Model 2		Model 3	
	W	σ	W	σ	W	σ
W^{Gt}_{MgFe}	0		Asymmetric		Asymmetric	
$W^{Gt}_{Fe\text{-}Mg}$	—		835**		695†	420
$W^{Gt}_{Mg\text{-}Fe}$	—		10460**	2092	2115†	295
ΔW^{Gt}_{Mn}	5485*	745	18975*	818	8231*	680
W^{Gt}_{MnFe}	1800‡		1800‡		1800‡	
W^{Gt}_{MnMg}	3685*		17175*		6431*	
All models:						
	W				σ	
W^{Gt}_{Ca}	12550**				2090	
W^{Bt}_{MgFe}	0					
W^{Bt}_{Ti}	0 or −31200				5000§	
$\Delta W^{Bt}_{Al,VI}$	0 or −6600§				(?)	

* This work.
** Ganguly and Saxena (1984); Geiger et al. (1987).
† Hackler and Wood (1989).
‡ O'Neill et al. (1989).
§ Indares and Martignole (1985).

the two interaction parameters is linear for each area:

$$\Delta W^{Grt}_{Mn} = 1.45 W^{Grt}_{MgFe} + 4580 \quad \text{(Rio Mora)} \quad (8)$$

$$\Delta W^{Grt}_{Mn} = 1.46 W^{Grt}_{MgFe} + 3930 \quad \text{(Pecos Baldy)} \quad (9)$$

$$\Delta W^{Grt}_{Mn} = 0.80 W^{Grt}_{MgFe} + 11164 \quad \text{(Cerro Colorado).} \quad (10)$$

These relationships incorporate all of the multicolinearities discussed above, and their differences probably reflect variations in temperature, pressure, bulk composition, or degree of retrogression. As noted above, the data from Cerro Colorado, in particular, may have been affected to a small extent by retrogression or alteration. Assuming that ΔW^{Grt}_{Mn} and W^{Grt}_{MgFe} are independent of temperature, the slopes and intercepts from the three equations can be regressed against each other to suggest the unique values of ΔW^{Grt}_{Mn} and W^{Grt}_{MgFe}. Such a regression yields 19400 and 10400 J/mol for ΔW^{Grt}_{Mn} and W^{Grt}_{MgFe}, respectively. The value of W^{Grt}_{MgFe} (10400 J/mol) is remarkably consistent with the asymmetric mixing model of Ganguly and Saxena (1984) and Geiger et al. (1987), whose models yield values on the order of 10000 J/mol for the garnet compositions presented here. The value of ΔW^{Grt}_{Mn} (19400 J/mol) is slightly larger than that suggested by Ganguly and Saxena (1984) and may, in part, reflect the fact that the biotite samples were generally not corrected for Fe^{3+} in the data sets that they regressed.

We realize that these mixing parameters are not well constrained; they are defined primarily by differences between Cerro Colorado and the other two map areas. We interpret the results to suggest that a nonideal Mg-Fe mixing model may be preferable to an ideal one, but we suspect that the large value of W_{MgFe} may have, in part, resulted from scatter in the Cerro Colorado data. We suggest that this methodology could be applied to garnet-biotite pairs from numerous other study areas in order to obtain unique and realistic estimates of W^{Grt}_{MgFe} and ΔW^{Grt}_{Mn}. One of us (Williams) has begun such an analysis, which requires knowing the complete chemistry of garnet and biotite, including Fe^{3+}/total Fe, for a suite of samples with a limited range in T and P, data not commonly available in the literature.

Suggested mixing parameters

Data from this study permit three sets of mixing parameters for garnet (and biotite) in the Mn-Mg-Fe system (Table 10). Model 1 assumes ideal Mg-Fe mixing in garnet and biotite. The assumption leads to the minimum possible value for ΔW^{Grt}_{Mn}, 5500 (±750) J/mol (one-site basis). Model 2 uses the Mg-Fe mixing model of Ganguly and Saxena (1984). This model leads to a large estimate of ΔW^{Grt}_{Mn} (19000 ± 800 J/mol), and almost certainly represents a maximum estimate for this parameter. Model 3 uses the Mg-Fe mixing model of Hackler and Wood (1989) and leads to an intermediate estimate of ΔW^{Grt}_{Mn} (8200 ± 700 J/mol). Because this model seems to characterize Mg-Fe mixing at high X_{alm} better than that of Ganguly and Saxena (1984) (see discussion in Hackler and Wood, 1989), we prefer this model.

O'Neill et al. (1989) concluded that W^{Grt}_{MnFe} is approximately 1800 J/mol based on the partitioning of Mn between garnet and ilmenite. Based on this value, W^{Grt}_{MnMg} is approximately 3700, 17200, and 6400 J/mol for Models 1, 2, and 3, respectively (Table 10). Again, we prefer the third estimate. Consistent with predictions, Mn-Mg mixing is significantly less ideal than Fe-Mn mixing.

IMPLICATIONS FOR GARNET-BIOTITE GEOTHERMOMETRY

Geothermometry in the Mn,Ca-free system

Many studies have derived useful temperature estimates by applying the Ferry and Spear (1978) experimental calibration to rocks low in Mn and Ca, even though the calibration does not treat nonideal mixing in garnet. We have applied their calibration directly to specimens from New Mexico in which garnets have low Mn and Ca, yielding temperatures consistent with those of coexisting aluminum silicate assemblages (Grambling and Williams, 1985; Grambling, 1986). If Mg and Fe do not mix ideally in garnet and if the Fe^{3+}/Fe^{2+} ratio of biotite is variable, then one must question why the Ferry-Spear calibration of the geothermometer works so well.

Garnet and biotite in the low-Mn, low-Ca rocks from New Mexico have compositions close to those in the Ferry and Spear experiments with $(X_{alm} - X_{prp})$ near 0.80 and $Fe^{3+}/(Fe^{2+} + Fe^{3+})$ in biotite near 0.10. At this composition, the calibration and the field data are affected equally by nonideal Mg-Fe mixing in garnet and by Fe^{3+} in biotite. From the relationships in Figures 3 and 5, it seems likely that most relatively reduced, amphibolite-facies garnets that are low in X_{sps} and X_{grs} have similar values of $(X_{alm} - X_{prp})$. The compositional similarity appears to explain the success of the Ferry and Spear calibration.

Fe^{3+} in biotite

All available data (this study; Goldman and Albee, 1977; Wones and Eugster, 1965; M. Darby Dyar, personal communication) show that biotite can contain significant Fe^{3+} and that the Fe^{3+}/Fe^{2+} ratio of biotite is quite variable. Consequently, accurate garnet-biotite geothermometry using microprobe data must employ biotite compositions corrected for Fe^{3+}. Corrections for Fe^{3+} may be made directly using Mössbauer or wet-chemical analyses. Alternatively, the relations among biotite and compositions of Fe-Ti oxide (Fig. 2) can be used to estimate Fe^{3+} in biotite.

For accurate geothermometry, it is also necessary to estimate the amount of Fe^{3+} in the biotite used by Ferry and Spear (1978). They did not measure Fe^{3+} in their experimental biotite but conducted their experiments in the presence of graphite and methane. If graphite equilibrated with methane at the P and T of the experiments, f_{O_2} should have been below those of the quartz-fayalite-magnetite (QFM) buffer (Eugster and Skippen, 1967; Chou, 1987). All biotite samples analyzed in this study appear to have crystallized at f_{O_2} above QFM (Grambling, 1986). Thus, the experimental biotite should have had $Fe^{3+}/(Fe^{3+} + Fe^{2+})$ below 0.12, the most-reduced biotite from New Mexico. Wones and Eugster (1965) and Dyar (personal communication, 1989) suggested that some Fe^{3+} is present in virtually all biotite. We estimate that the biotite used by Ferry and Spear had $Fe^{3+}/(Fe^{3+} + Fe^{2+})$ near 0.10.

An empirical garnet-biotite thermometer for Mn-Fe-Mg garnets

Ferry and Spear's (1978) calibration of the garnet-biotite geothermometer was derived for the Fe-Mg system assuming that Fe and Mg mix ideally and that all Fe was Fe^{2+}. Their calibration can be modified to incorporate Fe-Mg nonideality (following Ganguly and Saxena, 1984) and to exclude Fe^{3+}:

$$\begin{aligned} RT \ln K_{eq} = &-17042 - 79.5(P) \\ &+ RT[0.782 - \ln (Fe^{2+}/Fe^{Tot})^{Bt*}] \\ &+ [(X_{prp} - X_{alm})(W_{MgFe})^{Grt*} \\ &- (X_{Fe} - X_{Mg})(W_{MgFe})^{Bt*}]/R \end{aligned} \quad (11)$$

where P is in kbar, T is in K, R in J/mol K, and the starred terms refer to the composition used in the calibration experiments. Garnets used by Ferry and Spear

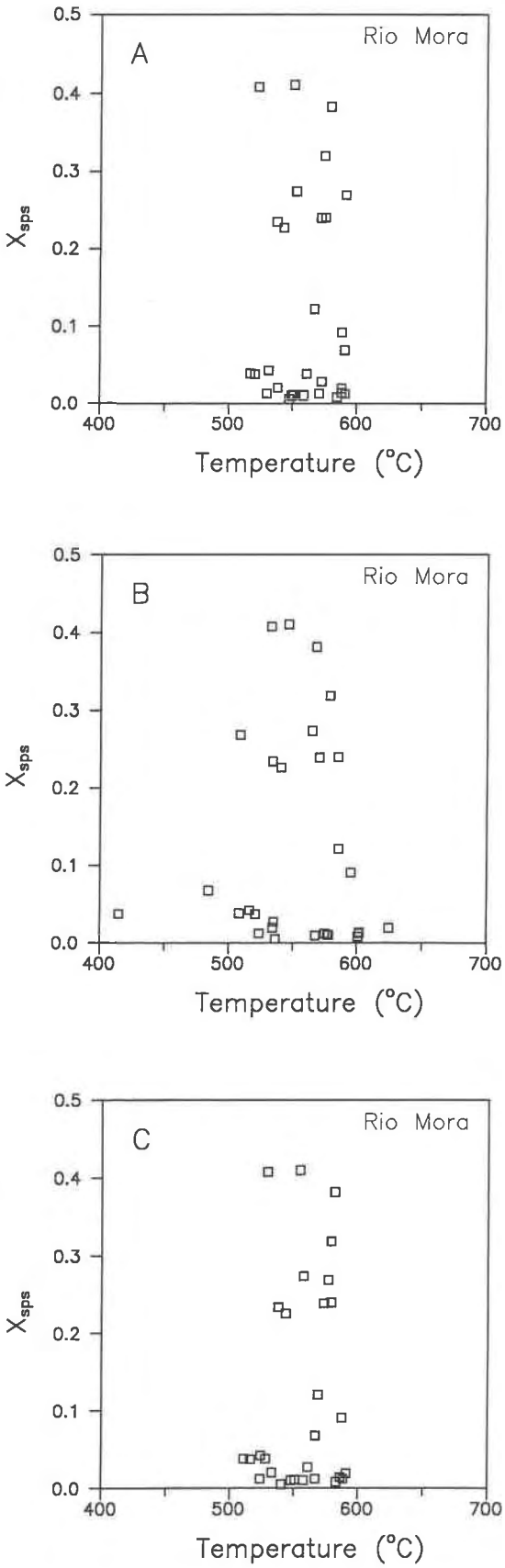

Fig. 11. Mole-fraction Mn in garnet vs. garnet-biotite temperature for samples from Rio Mora, New Mexico, calculated using Equation (12). (**A**) Temperatures calculated using interaction parameters from Table 10, Model 1, one Mn-dependent parameter. (**B**) Temperatures calculated using interaction parameters from Table 10, Model 2, nonideal Fe-Mg mixing in garnet, based on Ganguly and Saxena (1984). (**C**) Temperatures calculated using interaction parameters from Table 10, Model 3, nonideal Fe-Mg mixing in garnet, based on Hackler and Wood (1989).

TABLE 11. Geothermometry (°C)

Rio Mora (P = 4.5 kbar)					Pecos Baldy (P = 3.8 kbar)				
		Model					Model		
Sample	ln K_D	1	2	3	Sample	ln K_D	1	2	3
81-23a	−1.930	539	528	537	77-85B	−1.993	518	540	522
80-142	−1.788	577	592	580	76-420	−2.034	502	507	503
80-46	−1.902	541	559	545	77-125	−2.154	491	484	490
80-46b	−1.874	551	569	554	77-15	−2.020	518	547	523
C81-174	−1.961	543	569	548	77-81E	−1.973	527	541	530
80-30	−1.847	563	566	563	77-103	−2.058	499	534	505
80-43	−1.782	583	593	585	76-400B	−2.188	485	475	483
80-187	−2.010	522	515	521	77-41	−2.177	482	488	483
80-42	−1.780	580	593	583	76-446	−2.154	488	494	489
80-20	−1.790	581	616	587	77-39	−2.139	488	501	490
80-51	−2.001	531	525	530	77-6	−2.001	527	545	530
C81-181	−1.891	566	525	558	77-42	−2.091	508	523	511
80-178a	−2.046	514	511	513	76-445	−2.103	488	542	498
81-225	−1.976	554	404	525	78-22A	−2.063	504	567	516
80-18a	−2.113	511	499	508	77-73	−2.134	493	514	497
80-192-2	−2.094	525	507	521	77-23	−2.187	484	553	497
81-234sC	−1.894	585	473	563	83-45	−2.187	487	531	496
C81-148	−1.898	584	584	584	77-46D	−2.181	521	508	518
C81-105	−2.042	564	574	565	84-163-2	−2.209	514	501	512
C?81-213	−2.129	543	526	540	84-163-1	−2.195	516	502	513
81-13a	−2.257	538	519	534	84-169-2	−2.269	505	493	502
C81-310	−2.028	573	555	570	76-437	−2.167	523	581	535
80-178	−2.033	577	570	575	84-169A	−2.223	520	511	518
81-145	−2.077	594	492	573	76-400	−2.219	521	514	520
81-70a	−2.100	555	549	554	78-25	−2.208	527	523	526
80-218	−2.084	579	561	575	76-379	−2.302	503	499	502
82-62	−2.168	586	549	578	77-45	−2.240	525	523	524
C81-244	−2.326	529	514	526	84-162-2	−2.403	509	495	506
82-12	−2.215	558	526	551	84-162-1	−2.373	510	495	507
	Mean	557	540	553		Mean	506	518	508
	σ	24	43	24		σ	15	25	14

had $(X_{prp} - X_{alm}) = 0.8$ and, based on the discussion above, $(Fe^{2+}/Fe^{Tot})^{Bt*}$ may have been approximately 0.90.

Equation 11 can be combined with Equation 5 to yield a general expression for the nonideal geothermometer:

$$T(\mathrm{K}) = [-17042 - 79.5(P) + 0.8W^{Grt*}_{MgFe} - W_{MgFe}(X_{alm} - X_{prp}) - \Delta W^{Grt}_{Ca}(X_{grs})^{Grt} - \Delta W^{Grt}_{Mn}(X_{sps})^{Grt} + \Delta W^{Bt}_{Ti}(X_{Ti})^{Bt} - \Delta W^{Bt}_{Al6}(X_{A16})^{Bt}] \div R[\ln K_D - 0.782 + \ln (Fe^{2+}Bt/Fe^{Tot,Bt})^*] \quad (12)$$

where K_D includes only Fe^{2+} and, as above, starred terms refer to the composition of the minerals in the calibration experiments. This form of the geothermometer assumes that Mg-Fe and Mn mixing are ideal in biotite but allows for nonideal mixing of octahedral Ti, Al, and Fe^{3+}.

Substitution of the three sets of interaction parameters for Mn-Fe-Mg mixing (Table 10) into Equation 12 leads to three expressions of the geothermometer. All three forms treat only Fe^{2+} in biotite. The first, using mixing Model 1 (Table 10), is relatively simple; all mixing terms are excluded except those for Mn and Ca in garnet. Essentially, this relies on the correlations between X_{sps}, $(X_{alm} - X_{prp})$, and $(X_{Fe} - X_{Mg})^{Bt}$, in order to place all interrelated nonideality artificially into a single X_{sps}-dependent parameter. Because of this limitation, it can be applied only to suites of rocks with linear relationships among the compositional parameters similar to those seen here. Fortunately, to a first approximation, these relationships are common. The small magnitude of the X_{sps}-dependent parameter (5500 J/mol) is consistent with the observation that at relatively low X_{sps}, the assumption of ideal Mn and Mg-Fe mixing does not produce dramatically erroneous results (Hodges and Spear, 1982; Williams and Grambling, 1984).

The two remaining expressions of the thermometer explicitly incorporate nonideal Mg-Fe mixing in garnet (Table 10, Models 2 and 3). W^{Grt}_{FeMg} is calculated using Equation 4. W^{Grt*}_{MgFe} is 9500 J/mol for Model 2 and 2000 J/mol for Model 3. Terms characterizing nonideal Ti and Al mixing in biotite can be inserted into both equations if W^{Bt}_{Ti} and W^{Bt}_{Al} are known. As noted above, mixing Model 3 (Table 10) is our preferred model at present, and thus, our preferred geothermometer for Mn-Fe-Mg garnets is

$$T(\mathrm{K}) = [-17042 - 79.5(P) + 1579 - W_{MgFe}(X_{alm} - X_{prp}) - 12550(X_{grs}) - 8230(X_{sps})] \div R[\ln K_D - 0.782 + \ln (0.90)]. \quad (13)$$

We have applied the three forms of the garnet-biotite geothermometer to specimens from New Mexico, with biotite corrected for Fe^{3+} using the correlation between Fe^{3+} in biotite and $X_{Fe_2O_3}$ in hematite-ilmenite solid solution (Table 11). Mean temperatures are within error for the three thermometers, and all are compatible with in-

TABLE 11.—*Continued*

Cerro Colorado (P = 4.5 kbar)					Rio Mora high-Mn samples, not used in regression analyses				
		Model					Model		
Sample	ln K_D	1	2	3	Sample	ln K_D	1	2	3
W83-302	−1.689	634	529	613	84-147e	−2.166	632	610	626
W84-35	−2.290	467	495	472	84-147d	−2.123	639	631	637
W84-86	−2.154	530	435	511	81-221	−2.064	723	782	734
W84-94b	−2.278	489	513	494	81-175a	−2.075	716	797	730
W84-117a	−1.834	645	611	638	81-139	−1.302	1070	1208	1092
W84-130a	−2.176	523	527	524	81-139a	−1.182	1155	1307	1179
W83-300	−1.816	662	614	652					
W84-145b	−2.251	503	526	507					
W85-195b	−2.231	519	526	520					
W84-58	−2.094	560	561	560					
W84-153b	−2.164	539	521	536					
W84-87	−2.184	535	544	537					
W85-253	−1.962	612	569	604					
W84-75	−2.334	494	490	493					
W83-242	−2.172	544	549	545					
W84-133	−2.391	484	493	485					
W85-254	−2.283	541	547	542					
	Mean	546	532	543					
	σ	57	42	52					

dependent estimates of the peak metamorphic temperature. The data from Rio Mora are plotted in Figure 11 as an illustration. The standard deviations are generally larger for Model 2 than for Model 3. For example, data from Rio Mora yield 560 °C ± 24 (σ), 543 °C ± 43 (σ), and 557 °C ± 24 (σ) for Models 1, 2, and 3, respectively. As discussed above, the increased standard deviation for temperatures calculated using Model 2 probably reflects the increased sensitivity of this model to minor compositional variation. Although within the limits of error, the Cerro Colorado mean temperature is somewhat less than predicted, and the standard deviation is considerably larger than expected, presumably reflecting retrograde resorption or reequilibration.

We suggest limiting these thermometers to garnets with X_{sps} less than 0.50, X_{grs} less than 0.10, and biotite with compositions similar to those reported here. Significant variations in Ti and Al, either within a data set or between the data set and the biotite used for these calibrations, may affect calculated temperatures. Variations in Ti and Al in biotite seem to be most extreme at temperatures above 650 °C, which may place an upper limit on the calibrated thermometer presented herein.

Theoretical uncertainties for the three forms of the geothermometer were calculated using the methodology of Powell (1985) and Powell and Holland (1988). Although strong correlations exist among the compositional parameters, errors associated with the compositional data were assumed to be essentially uncorrelated. As expected, the calculated uncertainties vary significantly as a function of composition and as a function of the chosen mixing model. For Model 1, uncertainties range from 25 ° for low-Mn samples to 35 ° for high-Mn samples (X_{sps} = approximately 0.40). For Model 2, uncertainties range from 35 ° for low-Mn samples to 65 ° for high-Mn samples. For Model 3, uncertainties range from 25 ° for low-Mn samples to 45 ° for high-Mn samples. These estimated uncertainties are generally consistent with the calculated standard deviations for the three New Mexico data sets (Table 11).

ACKNOWLEDGMENTS

This research was supported by NSF grant EAR-8309503 to J.A. Grambling at the University of New Mexico, and funding for the electron microprobe at the University of New Mexico was provided under NSF grant EAR-8201211. We gratefully acknowledge R. Burns and M. Darby Dyar for providing Mössbauer analyses and M. Darby Dyar for helpful discussions. Helpful comments were provided by T. Hoisch, J. Lieberman, and S. Seaman. The manuscript was greatly improved by reviews by F. Spear, J. Ganguly, M. Kohn, and an anonymous reviewer.

REFERENCES CITED

Anovitz, L.M., and Essene, E.J. (1987) Phase equilibria in the system $CaCO_3$-$MgCO_3$-$FeCO_3$. Journal of Petrology, 28, 389–414.

Belsley, D.A., Kuh, A., and Welsh, R.E. (1980) Regression diagnostics: Identifying influential data and sources of colinearity. Wiley, New York.

Chinner, G.A. (1960) Pelitic gneisses with varying ferrous/ferric ratios from Glen Cova, Angus, Scotland. Journal of Petrology, 1, 178–217.

Chou, I-Ming (1987) Calibration of the graphite-methane buffer using f_{H_2} sensors at 2-kbar pressure. American Mineralogist, 72, 76–81.

Dahl, P.S. (1980) The thermal-compositional dependence of Fe^{2+}-Mg^{2+} distributions between coexisting garnet and clinopyroxene: Applications to geothermometry. American Mineralogist, 65, 852–866.

Dallmeyer, R.D. (1974) The role of crystal structure in controlling the partitioning of Mg and Fe^{2+} between coexisting garnet and biotite. American Mineralogist, 59, 201–203.

Devore, J.L. (1982) Probability and statistics for engineering and the sciences. Brooks/Cole Publishing Company, Monterey, California, 640 p.

Eugster, H.P., and Skippen, G.B. (1967) Igneous and metamorphic reactions involving gas equilibria. In P.H. Abelson, Ed., Researches in Geochemistry, vol. 2. Wiley, New York.

Ferry, J.M. (1980) A comparative study of geothermometers and geobarometers in pelitic schists from south-central Maine. American Mineralogist, 65, 720–732.

Ferry, J.M., and Spear, F.S. (1978) Experimental calibration of the partitioning of Fe and Mg between biotite and garnet. Contributions to Mineralogy and Petrology, 66, 113–117.

Ganguly, J., and Kennedy, G.C. (1974) The energetics of natural garnet solid solution. I. Mixing of aluminosilicate end-members. Contributions to Mineralogy and Petrology, 48, 137–148.

Ganguly, J., and Saxena, S.K. (1984) Mixing properties of aluminosilicates garnets: Constraints from natural and experimental data, and applications to geothermo-barometry. American Mineralogist, 69, 88–97.

——— (1987) Mixtures and mineral reactions. Springer-Verlag, New York, 291 p.

Geiger, C.A., Newton, R.C., and Kleppa, O.J. (1987) Enthalpy of mixing of synthetic almandine-grossular and almandine-pyrope garnets from high-temperature solution calorimetry. Geochimica et Cosmochimica Acta, 51, 1755–1763.

Goldman, D.S., and Albee, A.L. (1977) Correlation of Mg/Fe partitioning between garnet and biotite with $^{18}O/^{16}O$ partitioning between quartz and magnetite. American Journal of Science, 277, 750–767.

Grambling, J.A. (1986) A regional gradient in the composition of metamorphic fluids in pelitic schist, Pecos Baldy, New Mexico. Contributions to Mineralogy and Petrology, 94, 149–164.

Grambling, J.A., and Williams, M.L. (1985) The effects of Fe^{3+} and Mn^{3+} on aluminum silicate phase relations in north-central New Mexico, U.S.A. Journal of Petrology, 26, 324–354.

Grambling, J.A., Williams, M.L., Smith, R.F., and Mawer, C.K. (1989) The role of crustal extension in the metamorphism of Proterozoic rocks in northern New Mexico. Geological Society of America Special Paper 235, 87–110.

Guggenheim, E.A. (1967) Thermodynamics. Elsevier/North Holland, New York.

Guidotti, C.V. (1984) Micas in metamorphic rocks. In S.W. Bailey, Ed., Micas. Mineralogical Society of America Reviews in Mineralogy, 13, 357–467.

Hackler, R.T., and Wood, B.J. (1989) Experimental determination of Fe and Mg exchange between garnet and olivine and estimation of Fe-Mg mixing properties in garnet. American Mineralogist, 74, 994–999.

Hodges, K.V., and Crowley, P.D. (1985) Error estimation and empirical geothermobarometry for pelitic systems. American Mineralogist, 70, 702–709.

Hodges, K.V., and Spear, F.S. (1982) Geothermometry, geobarometry and the Al_2SiO_5 triple point at Mt. Moosilauke, New Hampshire. American Mineralogist, 67, 1118–1134.

Hounslow, A.W., and Moore, J.M., Jr. (1967) Chemical petrology of Grenville schists near Fernleigh, Ontario. Journal of Petrology, 8, 1–28.

Hudson, N.F.C. (1985) Conditions of Dalradian metamorphism in the Buchan area, NE Scotland. Journal of the Geological Society of London, 142, 63–76.

Indares, A., and Martignole, J. (1985) Biotite-garnet geothermometry in the granulite facies: The influence of Ti and Al in biotite. American Mineralogist, 70, 272–278.

Mueller, R.F. (1972) Stability of biotite: A discussion. American Mineralogist, 57, 300–316.

Newton, R.C., and Haselton, H.T. (1981) Thermodynamics of the garnet-plagioclase-Al_2SiO_5-quartz geobarometer. In R.C. Newton, A. Navrotsky, and B.J. Wood, Eds., Thermodynamics of minerals and melts. Advances in Physical Geochemistry, 1, 129–145. Springer, New York.

O'Neill, H.St.C., Pownceby, M.I., and Wall, V.J. (1989) Activity-composition relations in $FeTiO_3$-$MnTiO_3$ ilmenite solid solutions from EMF measurements at 1050–1300 K. Contributions to Mineralogy and Petrology, 103, 216–222.

Phinney, W.C. (1963) Phase equilibria in the metamorphic rocks of St. Paul Island and Cape North Nova Scotia. Journal of Petrology, 4–1, 90–130.

Powell, R. (1985) Geothermometry and geobarometry: A discussion. Journal of the Geological Society of London, 142, 29–38.

Powell, R., and Holland, T.J.B. (1988) An internally consistent dataset with uncertainties and correlations: 3. Applications to geobarometry, worked examples and a computer program. Journal of Metamorphic Geology, 6, 173–204.

Rumble, D. III (1973) Fe-Ti oxide minerals from regionally metamorphosed quartzites of western New Hampshire. Contributions to Mineralogy and Petrology, 42, 181–195.

Sen, S.K., and Chakraborty, K.R. (1968) Magnesium-iron exchange equilibrium in garnet-biotite and metamorphic grade. Neues Jahrbuch für Mineralogie Abhandlungen, 108–2, 181–207.

Spear, F.S. (1988) Metamorphic fractional crystallization and internal metasomatism by diffusional homogenization of zoned garnets. Contributions to Mineralogy and Petrology, 99, 507–517.

St. Onge, M.R. (1984) Geothermometry and geobarometry in pelitic rocks of north-central Wopmay Orogen (early Proterozoic), Northwest Territories, Canada. Geological Society of America Bulletin, 95, 196–208.

Williams, M.L. (1987) Stratigraphic, structural, and metamorphic relationships in Proterozoic rocks from northern New Mexico. Ph.D. thesis, University of New Mexico, Albuquerque, 138 p.

Williams, M.L., and Grambling, J.A. (1984) Evidence of ideal solution of Fe, Mg, and Mn in garnet from northern New Mexico. Geological Society of America Abstracts with Programs, 16, 695.

Wones, D.R., and Eugster, H.P. (1965) Stability of biotite: Experiment, theory, and application. American Mineralogist, 50, 1228–1272.

Manuscript received June 3, 1988
Manuscript accepted May 25, 1990